Seasonal to interannual variability of vegetation and fires at SAFARI 2000 sites inferred from advanced very high resolution radiometer time series data

A. Anyamba,[1] C. O. Justice,[2] C. J. Tucker,[3] and Robert Mahoney[4]

Received 19 April 2002; revised 21 March 2003; accepted 5 May 2003; published 15 July 2003.

[1] NOAA advanced very high resolution radiometer data are used to place the SAFARI 2000 and SAFARI 1992 intensive campaigns in the context of the interannual variability of vegetation conditions in southern Africa. Normalized difference vegetation index (NDVI) measurements and sea surface temperature (SST) indices of El Niño/Southern Oscillation (ENSO) are compared and the connections explained. The paper shows the vegetation evolution for the 2000 growing season, with unprecedented high and persistent NDVI anomalies associated with a cold phase of ENSO (La Niña) and above average rainfall between November and May, south of 15°S. In contrast, the 1992 season showed marked negative NDVI anomalies associated with an extreme drought in the southern part of the region, associated with the warm phase of ENSO (El Niño). These differences in NDVI patterns resulted in different patterns of fire distribution. More satellite detections of active fires were observed in 2000 than in 1992, especially for Botswana, Namibia, southern Zimbabwe, and southern Mozambique. Comparisons between in situ airborne measurements collected in 2000 and 1992 require an understanding of the extremely different vegetation and fire conditions associated with those years. Generalizations from results of the two SAFARI campaigns should be made with careful consideration of the extreme differences in conditions and the large interannual variability encountered in southern Africa, as depicted by the long-term record of satellite vegetation measurements. *INDEX TERMS:* 1620 Global Change: Climate dynamics (3309); 1640 Global Change: Remote sensing; 1812 Hydrology: Drought; 9305 Information Related to Geographic Region: Africa; 4815 Oceanography: Biological and Chemical: Ecosystems, structure and dynamics; *KEYWORDS:* normalized difference vegetation index, El Niño, La Niña, fire dynamics, southern Africa, interannual climate dynamics

Citation: Anyamba, A., C. O. Justice, C. J. Tucker, and R. Mahoney, Seasonal to interannual variability of vegetation and fires at SAFARI 2000 sites inferred from advanced very high resolution radiometer time series data, *J. Geophys. Res.*, *108*(D13), 8507, doi:10.1029/2002JD002464, 2003.

1. Introduction

[2] Biomass burning is pervasive in southern Africa and is a common land management practice and a major biogeochemical process [*Frost*, 1998]. Two intensive international fieldwork campaigns have been undertaken in southern Africa over the last decade, fostering international collaborative research to study the interactions between biomass burning and atmospheric composition. The Southern African Regional Science Initiative 2000 (SAFARI 2000) was designed to study linkages between land-atmosphere processes and the relationship of biogenic, pyrogenic or anthropogenic emissions and consequences of their deposition to the functioning of the biogeophysical and biogeochemical systems of southern Africa (H. Annegarn et al., "The River of Smoke:" Characteristics of the southern African springtime biomass burning haze, submitted to *Journal of Geophysical Research*, 2003). Researchers undertook a number of ground, tower, aircraft and satellite based measurements of various parameters to achieve these goals. The program of measurements expanded on the experience gained and the data collected in SAFARI 1992 campaign [*van Wilgen et al.*, 1997].

[3] Southern Africa experiences considerable interannual climate variability. An understanding of interannual rainfall variability and its effect on vegetation dynamics in the region is required in order to compare different time measurements and for generalizations to be made from the research results. SAFARI 2000 was undertaken in an extremely wet year, which contrasts to the extremely dry conditions encountered during the SAFARI 1992. In this study, heritage normalized difference vegetation index (NDVI) time series data from the National Oceanic and

[1]Goddard Earth Science Technology Center, University of Maryland, Baltimore County and NASA Goddard Space Flight Center, Biospheric Science Branch, Greenbelt, Maryland, USA.
[2]Department of Geography, University of Maryland, College Park, Maryland, USA.
[3]NASA Goddard Space Flight Center, Biospheric Sciences Branch, Greenbelt, Maryland, USA.
[4]Global Science and Technology, Greenbelt, Maryland, USA.

0148-0227/03/2002JD002464$09.00

Atmospheric Administration (NOAA) advanced very high resolution radiometer (AVHRR) are used to provide a description of the patterns of seasonal to interannual variability for the region, with emphasis on the vegetation conditions and associated fires for 1992 and 2000.

2. Data and Analysis Methods

[4] The primary data set used in this study is the NDVI. This index is derived from broadband measurements in the visible and infrared portions of the electromagnetic spectrum made by the NOAA-AVHRR instrument. The index is calculated as:

$$\mathrm{NDVI} = (\rho_{\mathrm{nir}} - \rho_{\mathrm{r}})/(\rho_{\mathrm{nir}} + \rho_{\mathrm{r}}), \quad (1)$$

where ρ_r and ρ_{nir} are the surface reflectances in the 550–700 nm (visible) and 730–1000 nm (infrared) regions of the electromagnetic spectrum, respectively.

[5] High values of NDVI ($\sim +0.6$) are representative of dense green canopies, while low values ($\sim$0.1) are indicative of sparse vegetation cover. The index has been found to provide a strong vegetation signal and good spectral contrast from most background materials [*Tucker and Sellers*, 1986]. Seasonal variations in atmospheric water vapor [*Justice et al.*, 1991], atmospheric aerosol content [*Vermote et al.*, 1997] and large areas of bare soil in arid and semiarid areas may cause significant variations in NDVI not associated with actual vegetation cover [*Huete*, 1985]. However, on an aggregate basis, it has been shown to be a good indicator of various vegetation parameters, including green leaf area index (LAI), biomass, percent green cover, green biomass production and the fraction of absorbed photosynthetically active radiation [*Tucker*, 1979; *Asrar et al.*, 1984; *Sellers*, 1985]. Presented as a time series, the NDVI is a good indicator of vegetation phenology [*Townshend and Justice*, 1985]. A number of studies have shown that temporal variations in NDVI are associated with the seasonal dynamics of rainfall and evapotranspiration in a wide range of environmental conditions [*Gray and Tapley*, 1985; *Justice et al.*, 1986; *Nicholson et al.*, 1990; *Cihlar et al.*, 1991] and on global scale with atmospheric CO_2 fluxes. The compilation of more than 20 years of these data has resulted in more detailed studies of the biosphere-climate coupling. It is now possible to relate continental to regional-scale land surface response patterns to global-scale climatic perturbations, such as those forced by the El Niño/Southern Oscillation (ENSO) [*Eastman and Fulk*, 1993; *Myneni et al.*, 1996; *Anyamba and Eastman*, 1996]. In totality, NDVI can be used as an indicator of the biospheric response to climate variability at a range of spatial and temporal scales.

[6] Data used in this study were processed by the GIMMS group at NASA's Goddard Space Flight Center, as described by *Tucker et al.* [1994]. NDVI monthly data at 8 km spatial resolution were generated from 15-day composites using the maximum value compositing procedure to minimize effects of cloud contamination [*Holben*, 1986]. In addition, calibration based on invariant desert targets has been applied to the data to minimize the effects of sensor degradation [*Los*, 1993]. For this study, we subset the southern Africa region, covering 10°S–35°S, 10°E–40°E from the continental data set for the period July 1981–October 2000. From this time series, we created a long-term NDVI climatology by averaging data for all cloud-free pixels. We also calculated seasonal averages, long-term means and anomalies for four seasons defined as: December, January and February (DJF); March, April and May (MAM); June, July, and August (JJA); September, October and November (SON), as follows:

$$NDVI_{\sigma} = \left[\left((NDVI_{\alpha})/(NDVI_{\mu}) - 1\right)*100\right],$$

where $NDVI_\sigma$ are the respective seasonal percent anomalies, $NDVI_\alpha$ are individual season averages values and $NDVI_\mu$ are long-term means respectively. All averages and anomalies were calculated taking into account cloud and other quality control flags. This not only reduced the amount of data to be analyzed but also provides a clear picture of the interannual variability between different seasons for the years examined here.

[7] In addition, we created a combined rainfall data set for comparison with the NDVI time series data. The baseline rainfall data set used was extracted from Global Precipitation Climatology Project (GPCP) version 2 data set at 2.5° × 2.5° resolution [*Huffman et al.*, 1995]. The NOAA Climate Prediction Center (CPC) Africa Rainfall Estimate (RFE) data set version 1.0 and 2.0 for the period 1995–2001 at 10 × 10 km resolution [*Herman et al.*, 1997] supplemented this data set. In addition, the NASA/Tropical Rainfall Measuring Mission (TRMM) 3B43 data set at 1.0° × 1.0° resolution [*Adler et al.*, 2000] was used to fill missing RFE data for the period 1998–2000. These data were interpolated to the same 8 km Albers equal area projection grid for Southern Africa as that of NDVI. Long-term (1979–2001) and seasonal rainfall amounts were computed for the study region.

[8] The fire data used in this study was extracted from the SAFARI 2000 data archives (see http://www.safari2000.org/). The fire count data were derived from 3.9 μm channel of the NOAA AVHRR by identifying active fires during the satellite overpass [*Giglio et al.*, 1999]. Composite monthly fire count maps were created for the region based on daily fire counts at 8 km spatial resolution. A summary fire season map was created to show the geographic distribution of fires in the Southern Africa region during the study period.

[9] A number of study or "core" sites were used in SAFARI 2000 as a focus for intensive data collection. Six of these sites representing a range of vegetation types and climatic conditions were selected for detailed examination (Figure 1a, Table 1). For a 100 × 100 km box centered on each of these locations, we extracted data for the long-term monthly means, monthly NDVI and anomalies and corresponding rainfall and fire count data.

3. General Vegetation Patterns and Interannual Climate Dynamics

[10] Vegetation plays an important role in land-atmosphere interactions. Spatial variations in biomass production and the distribution and extent of fires have an impact on the type and amount of fire emissions [*Scholes et al.*, 1996]. Spatial and temporal variations in vegetation biomass are inherently linked to climate variability over the region. The general vegetation patterns are represented by the long-term

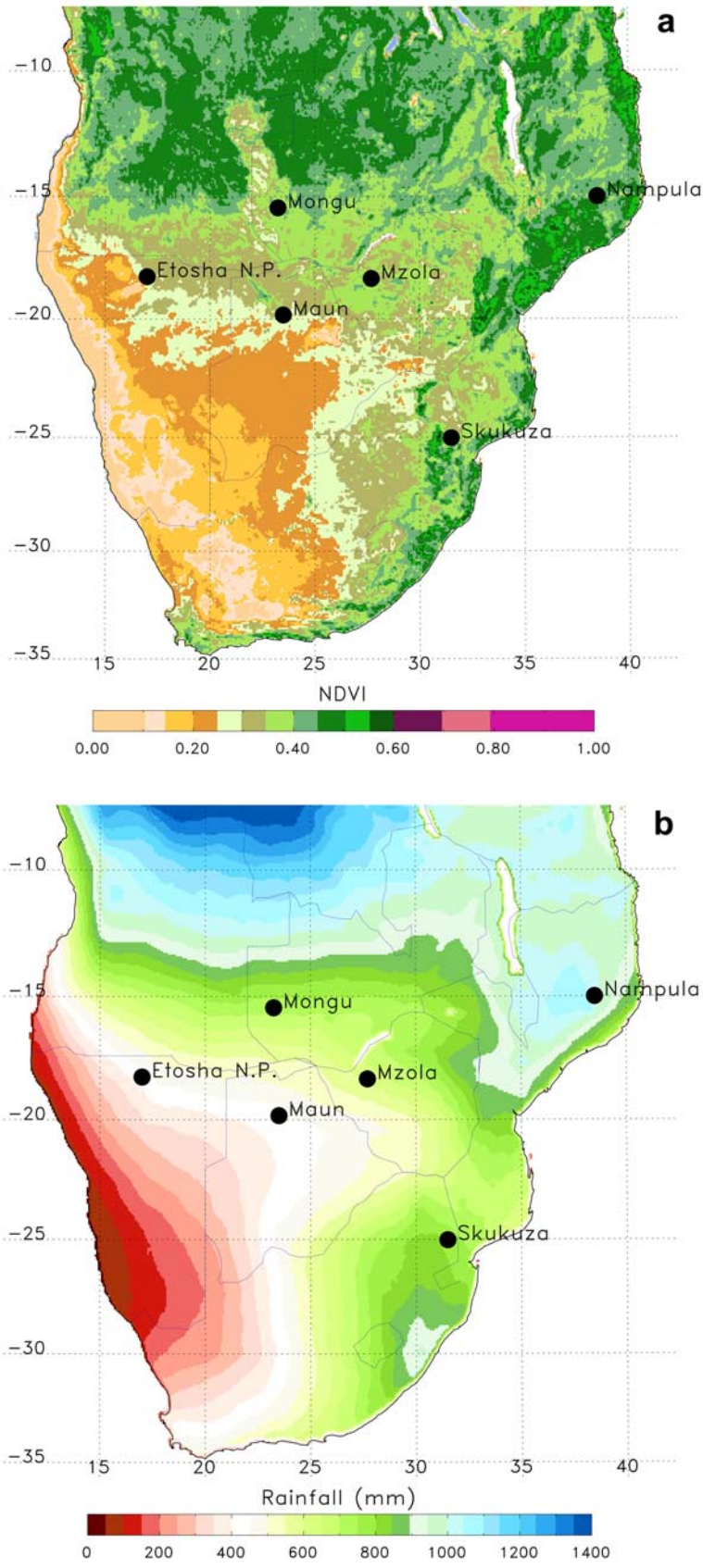

Figure 1. (a) Climatological mean NDVI (1982–2000) and (b) annual rainfall (1979–2000) for the southern Africa region and corresponding spatial patterns of average departure from long-term mean for (c) NDVI and (d) rainfall expressed as percentage. Locations of SAFARI 2000 sample validation sites are shown.

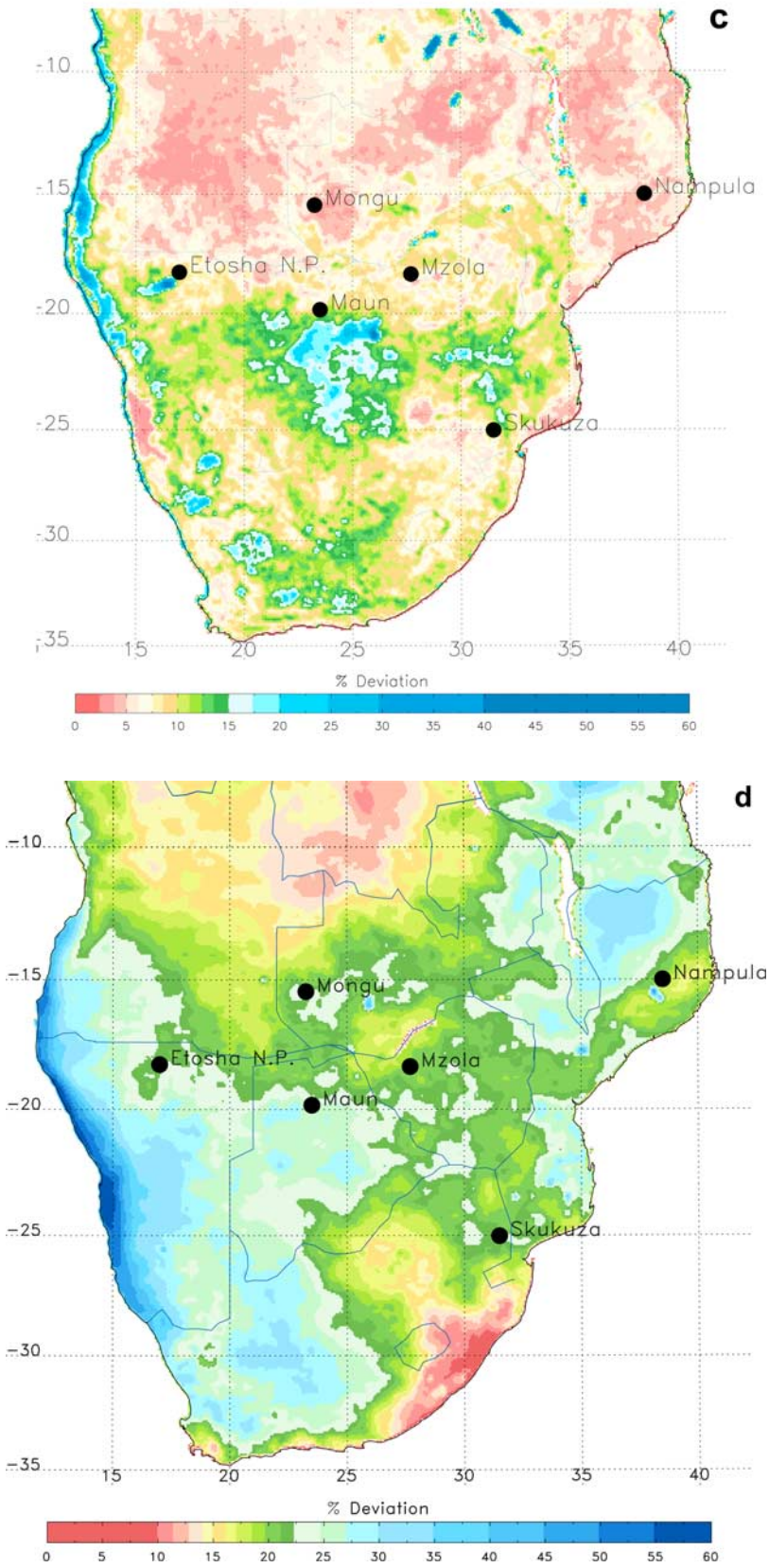

Figure 1. (continued)

Table 1. Location and Dominant Land Cover Types at Sample SAFARI 2000 Sites[a]

Site Name	Location, Latitude and Longitude	Annual Rainfall, mm	Rainfall Variation, %	Annual Mean NDVI	NDVI Variation, %	Dominant Land Cover Type(s)
Etosha National Park, Namibia	−18.00, 17.00	444	23	0.32	10	mopane woodland, dambo grassland, agriculture
Maun, Botswana	−19.83, 23.50	442	26	0.34	12	mopane and acacia woodland, riverine vegetation
Mzola, Zimbabwe	−18.33, 27.70	623	20	0.42	8.0	miombo and mopane woodland
Skukuza, Kruger NP, South Africa	−25.02, 31.50	786	22	0.44	10	combretum savanna and fine-leafed acacia savanna
Mongu, Zambia	−15.45, 23.25	810	19	0.44	6	woodland, dambo grassland, agriculture, floodplain
Nampula, Mozambique	−15.00, 38.50	1035	21	0.52	5	miombo woodland

[a]Land cover characterizations based on University of Maryland (UMD) Land Cover Classification for SAFARI 2000 Sites (see http://www.geog.umd.edu/landcover/cress/s2kchar.htm).

mean NDVI (1982–2000) map in Figure 1a. There is an east-west and southwest-northeast gradient in vegetation patterns. NDVI increases eastward from the west and northeastward from the southwest. These general patterns are related to the mean annual rainfall (Figure 1b) with areas in the west, for example in Namibia receiving <200 mm/year and those to in the east in Mozambique receiving ~700–1200 mm/year. This low rainfall has resulted in semiarid to desert conditions over much of the western half of the region, which is dominated by various types of savanna and open shrub lands. The eastern and northern parts of the region, which receive higher rainfall, are covered with more luxuriant miombo woodland formations.

[11] The variation in NDVI and rainfall is represented by the coefficient of variation expressed as percentage. This quantity is computed as the annual standard deviation divided by the long-term annual average for NDVI (1982–2000) and rainfall (1979–2000) respectively.

[12] The western half of the region, south of 17°S and west of 24°W exhibits the highest variability in rainfall, on the order of 20–30% as shown in Figure 1c. The areas to the north and northeastern parts of the region, which are much wetter, have lower variability in rainfall on the order of 10–15%. In contrast, the variation in vegetation as shown by percent departure in NDVI (Figure 1d) is lower than that of rainfall. The highest variability in NDVI occurs in areas south of 17°S, between 10 and 25%. The highest variation occurs in Botswana and along the northwestern coast of Namibia, and lowest variation occurs over the northern half of the region in central Angola, northern Mozambique and northern Zambia. The central and northern parts of the region are dominated by dense canopy miombo woodland formations where rainfall is not the main limiting factor on vegetation growth [*Fuller and Prince*, 1996; *Nicholson et al.*, 1990]. The general spatial patterns indicate that the variation in NDVI is approximately half that of rainfall. There is a close correspondence between variation in rainfall and NDVI for those areas with annual mean rainfall <600 mm/year and dominated by open savanna grasslands and woodlands.

[13] At the short timescale (2–7 years), the region is subject to extremes in interannual climate variability associated with the El Niño/Southern Oscillation phenomenon [*Janowiak*, 1988; *Ropelewski and Halpert*, 1996; *Lindsey*, 1988]. This is exemplified by a biennial tendency in rainfall fluctuations over the region at the short timescale [*Nicholson and Entekhabi*, 1986]. There is a tendency for below normal rainfall over the southern Africa region during the mature phase of warm ENSO events (Figure 2b), when the rainfall belt across the global tropics shifts eastward into the eastern equatorial tropical Pacific region [*Nicholson and Entekhabi*, 1986; *Ropelewski and Halpert*, 1996]. In general, during cold ENSO events, the rainfall belt shifts westward in the Pacific and correspondingly rainfall is enhanced over southern Africa. Recent studies indicate that normalized difference vegetation index (NDVI) data derived from the AVHRR can be used effectively to study the vegetation response patterns to this rainfall variability [*Myneni et al.*, 1996; *Anyamba and Eastman*, 1996; *Ricard and Poccard*, 1998; *Anyamba et al.*, 2001]. Figure 2 shows NDVI anomaly time series for Skukuza (25.02°S, 31.5°E) plotted against NINO3.4 SST, a sea surface temperature (SST) index drawn from the equatorial eastern Pacific Ocean (5°N–5°S, 170°–120°W) that shows the phase and magnitude of ENSO events. There is a temporal inverse relationship between NDVI anomalies and NINO 3.4 SST patterns ($r = 0.31$, $p < 0.05$). During warm events, there is a tendency for below normal NDVI (1982/1983, 1986/1987, 1994/1995) and above normal NDVI during cold events (1984/1985, 1988/1989, 1996/1997 and 1999/2000). Sometimes there are exceptions to these relationships, for example, the 1997/1998 warm event shows above normal NDVI. This is partially due to spatial differences in the land surface response patterns over the region from one ENSO event to another that may be controlled by regional meteorological mechanisms [*Walker*, 1990; *Jury et al.*, 1993; *Mason and Lindesay*, 1993; *Reason*, 2001]. Another interesting characteristic of the rainfall variability is the tendency for above normal rainfall during the early phase of a developing warm event and prevalence of drought during the mature phase of a warm event [see *Nicholson and Entekhabi*, 1986]. This pattern is spatially manifested in NDVI anomaly patterns, with a change from above normal NDVI during November–December to below normal NDVI during January–March of an ENSO warm event year [*Eastman and Anyamba*, 1996]. There is therefore a strong coupling between ENSO, rainfall variability and interannual vegetation dynamics of the region. In general, interannual climate variability in the region has a strong influence on green biomass production as inferred from satellite vegetation index measurements with a range of −40 to +40% between warm and cold events (Figure 2a). However, the spatial nature of this relationship is quite complex. As shown in Figure 2b, the strongest spatial correlations between rainfall

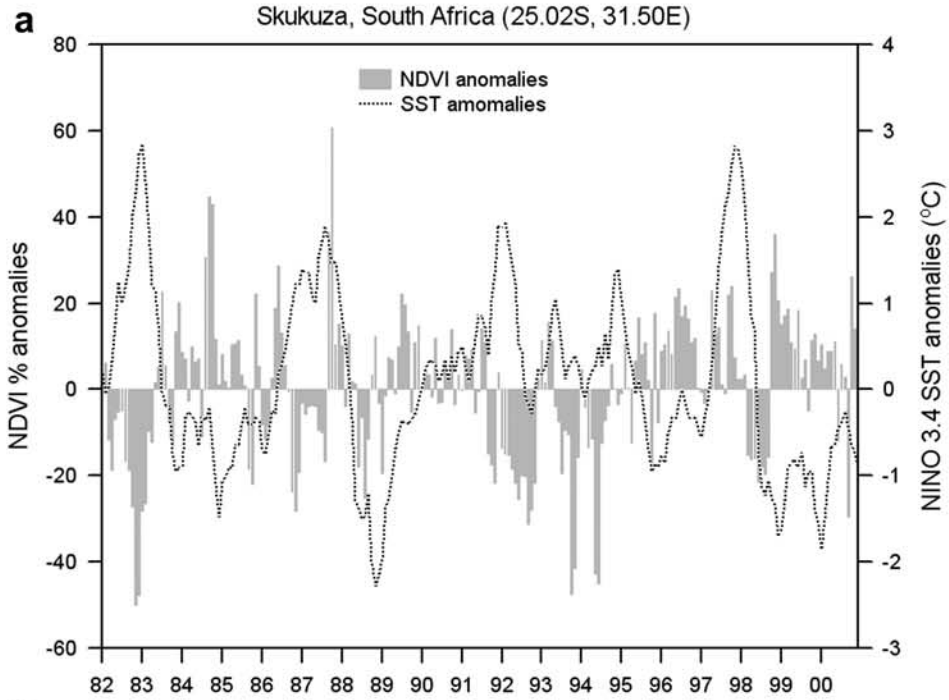
a
Skukuza, South Africa (25.02S, 31.50E)
NDVI anomalies
SST amomalies
NDVI % anomalies
NINO 3.4 SST anomalies (°C)
80
60
40
20
0
-20
-40
-60
4
3
2
1
0
-1
-2
-3
82 83 84 85 86 87 88 89 90 91 92 93 94 95 96 97 98 99 00

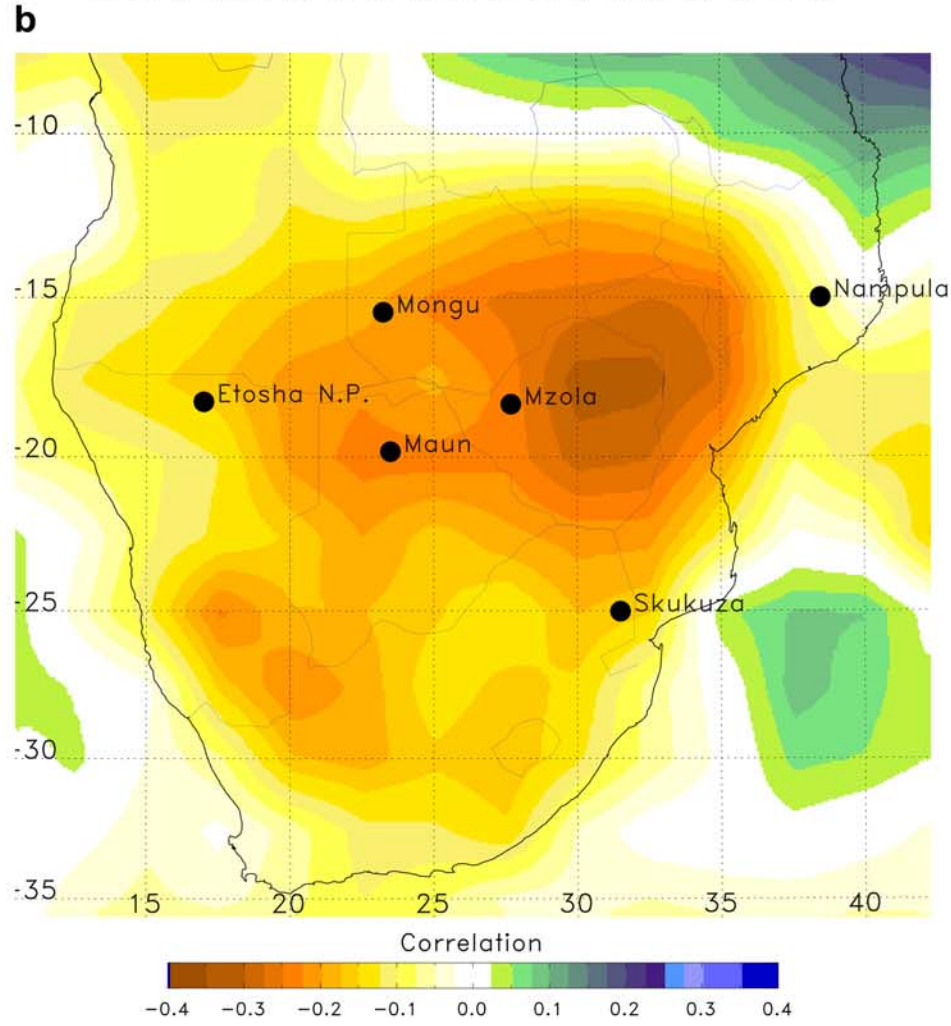
b
-10
-15
-20
-25
-30
-35
15
20
25
30
35
40
Mongu
Nampula
Etosha N.P.
Mzola
Maun
Skukuza
Correlation
−0.4 −0.3 −0.2 −0.1 0.0 0.1 0.2 0.3 0.4

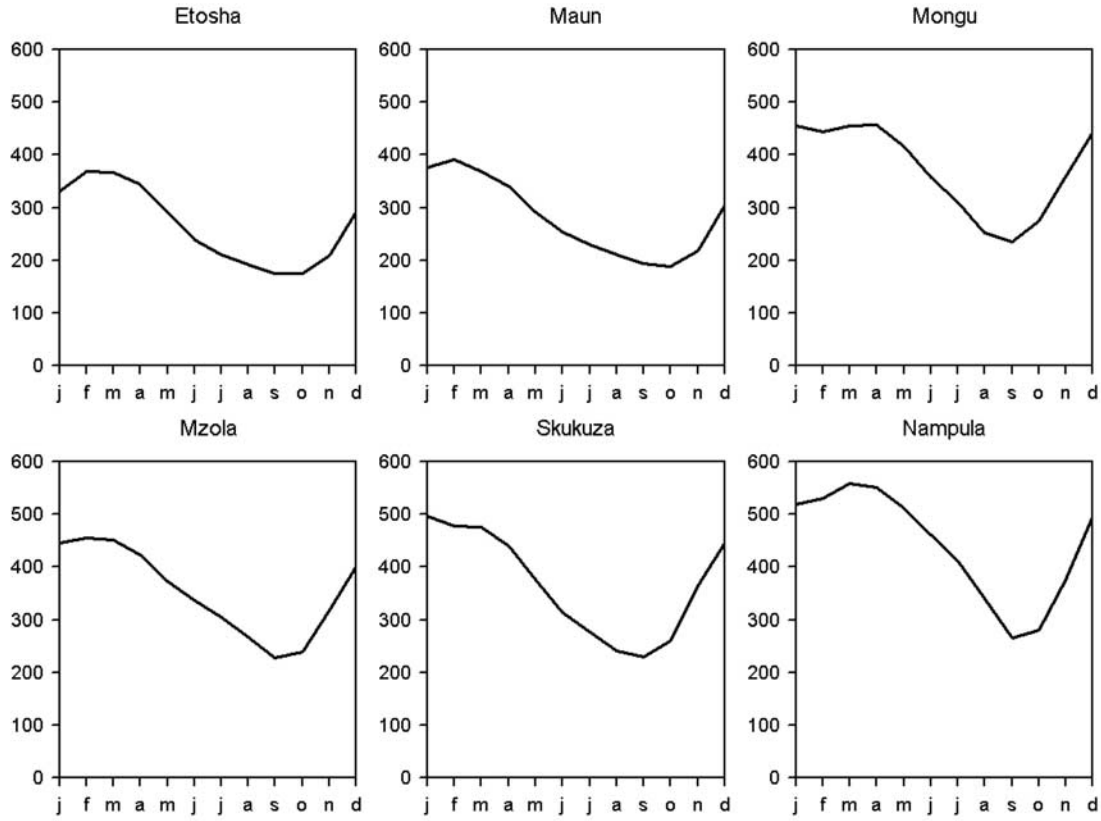

Figure 3. Mean annual evolution of NDVI (×1000) at SAFARI sample sites averaged for all years from 1982–1999. For all the selected sites, the maximum NDVI is reached during the southern summer peak rainfall season in January–March and the minimum during the winter (dry season) from June to October. Sites located in the arid region (e.g., Etosha, Maun) have longer dry season compared to the rest of the sites.

variability and NINO3.4 SST anomalies are for the eastern portion of the region below 15°S and east of 22°E. The relationship weakens northward becoming neutral to inverse for regions further north in northern Zambia and northeastern Mozambique into East Africa. As will be shown in this study, field studies during SAFARI 1992 and SAFARI 2000 both took place during periods of extreme variation in the climate regime with distinctly different vegetation dynamics.

4. Characteristics of Mean Annual NDVI Cycle at SAFARI 2000 Sites

[14] Figure 3 shows the mean annual cycle of NDVI for the six selected sites over the region. All the sites exhibit a unimodal distribution with a summer maximum and a winter minimum in NDVI. Generally, this annual mean trace of NDVI corresponds to the evolution of the rainfall season over the region. Rainfall generally migrates in concert with the location of the Intertropical Convergence Zone (ITCZ). The peak NDVI is reached in February–March for drier areas such as Etosha and Maun (~0.4), in March–May for wetter areas like Nampula and Mongu (~0.45–0.55), located further to the north and northeast, and in January for Skukuza (~0.55) located in the south-eastern part of the region. The vegetation-growing season is thus longer as one moves further north and northeast from the south-southwest. Topographic modifications to the rainfall amount and regime favor areas to the east with higher altitudes trapping and blocking moisture that would penetrate further west. The dry season is as long as five months for the dry areas from June to October, to as short as three months for wetter areas from August to October. The seasonal amplitude in NDVI is greater for the sites located in the wetter areas than for those in drier areas. There are however, variations to these patterns from year to year as governed by variability in rainfall amount and timing.

5. Evolution of the 1999/2000 Season

5.1. Regional Spatial Patterns

[15] Figure 4 shows the seasonal spatial evolution of NDVI patterns from December 1999 to November 2000

Figure 2. (opposite) (a) Temporal variations in NDVI anomalies for Skukuza, South Africa (July 1981–June 2000) plotted against ENSO index, NINO3.4 SST anomalies. There is a tendency for below (above) normal NDVI during warm (cold) ENSO events ($r = 0.31$, $p < 0.05$). (b) Summary correlation map between monthly NINO3.4 SST and rainfall anomalies for the period 1979–2000 illustrating the tendency for below (above) normal rainfall during El Niño (La Niña) events over the southern Africa region.

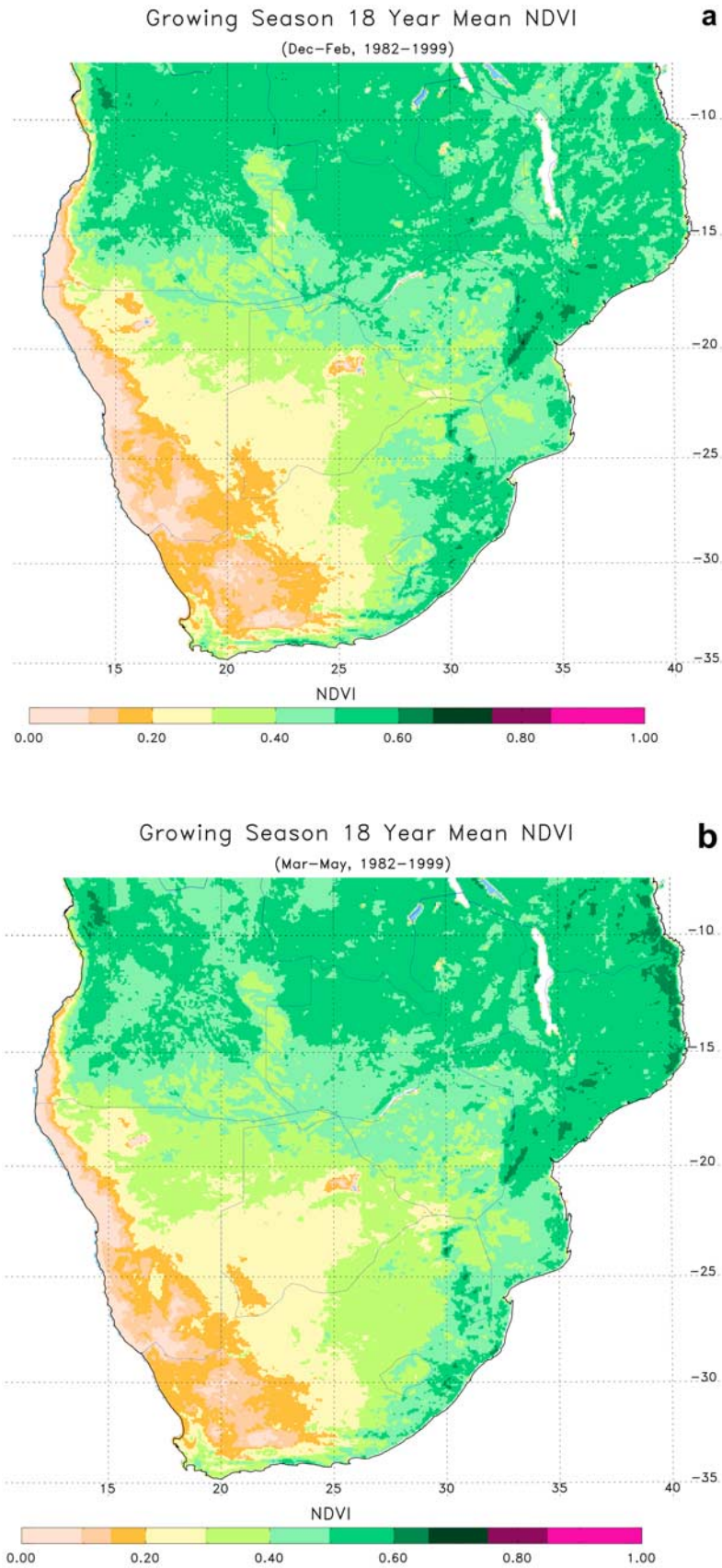

Figure 4. (a–d) Seasonal climatology NDVI maps for DJF, MAM, JJA, SON, corresponding (e–h) seasonal averages during the 1999/2000 season and (i–l) associated anomalies expressed as percent departures from respective climatologies.

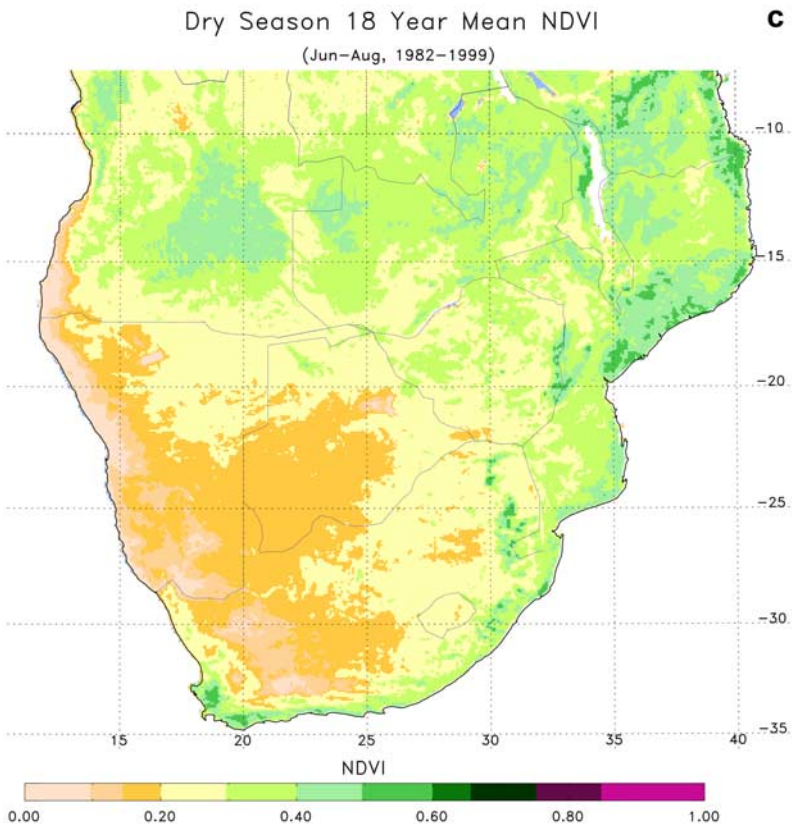

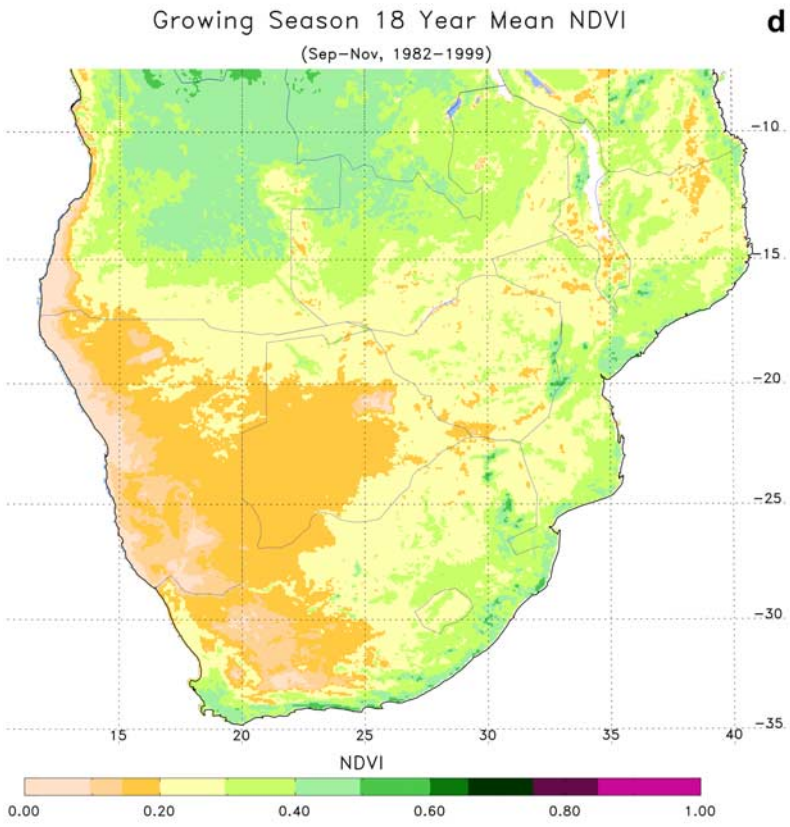

Figure 4. (continued)

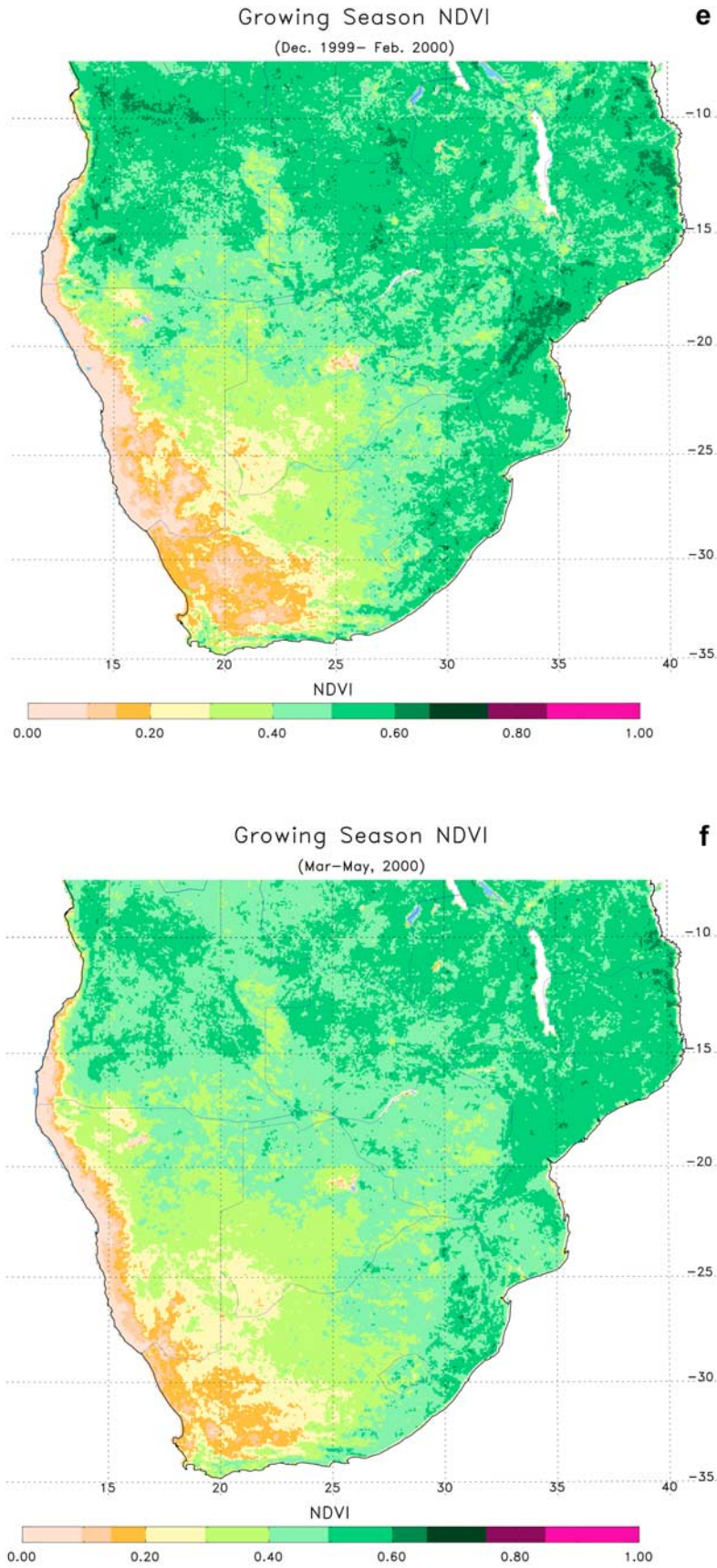

Figure 4. (continued)

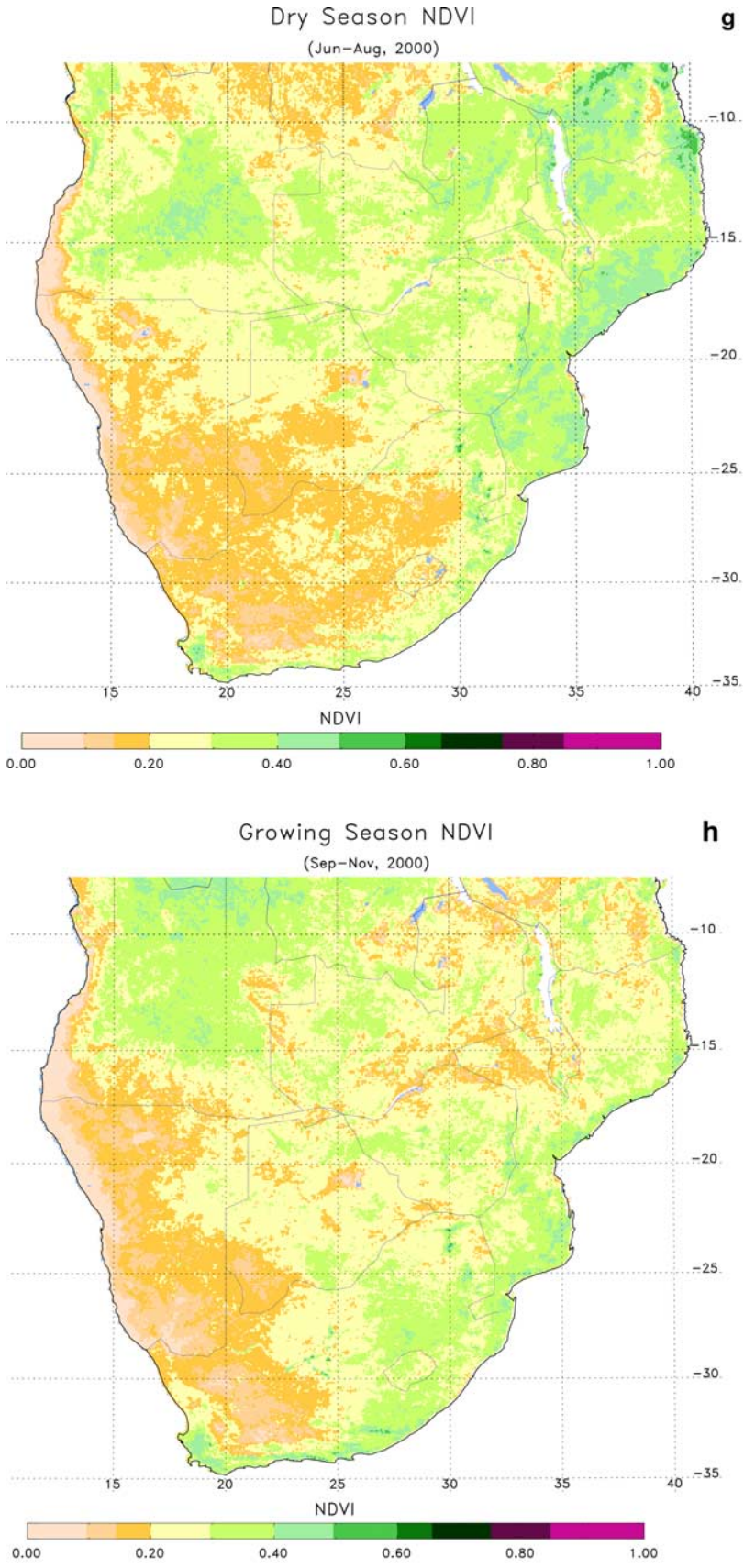

Figure 4. (continued)

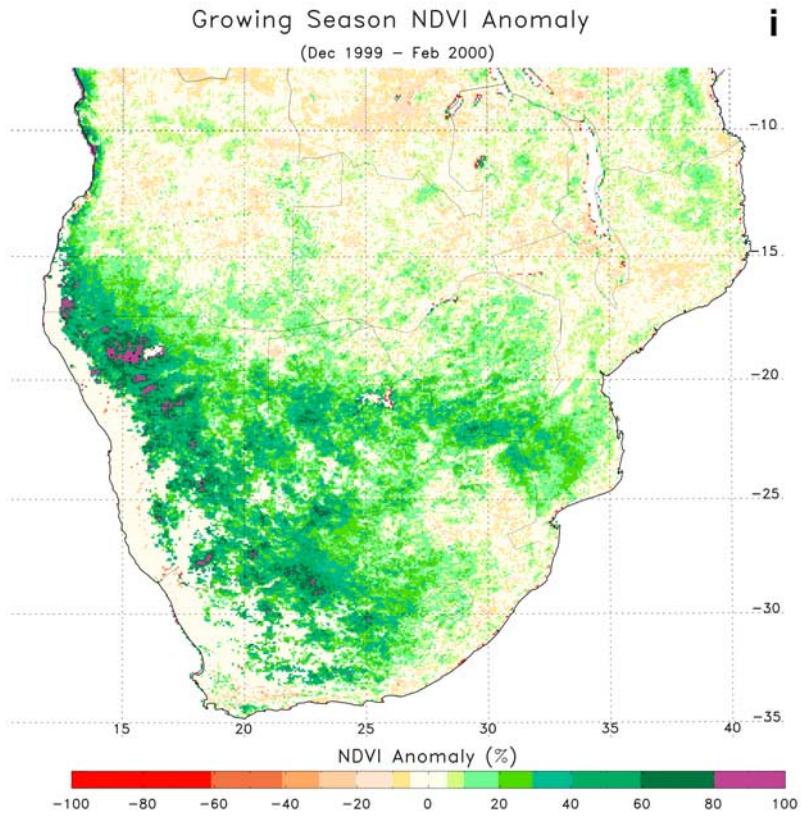

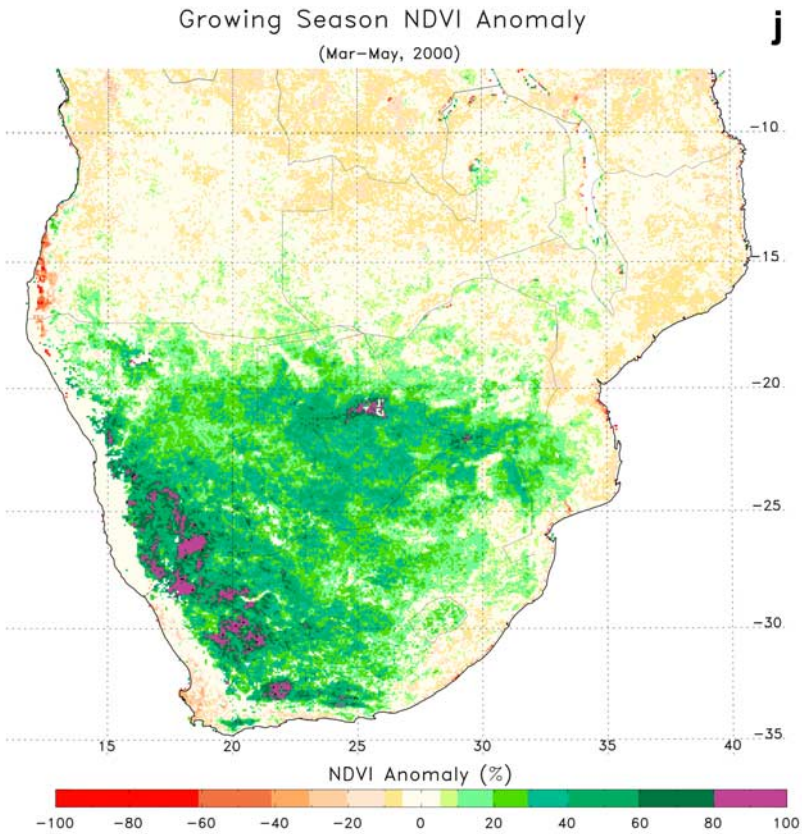

Figure 4. (continued)

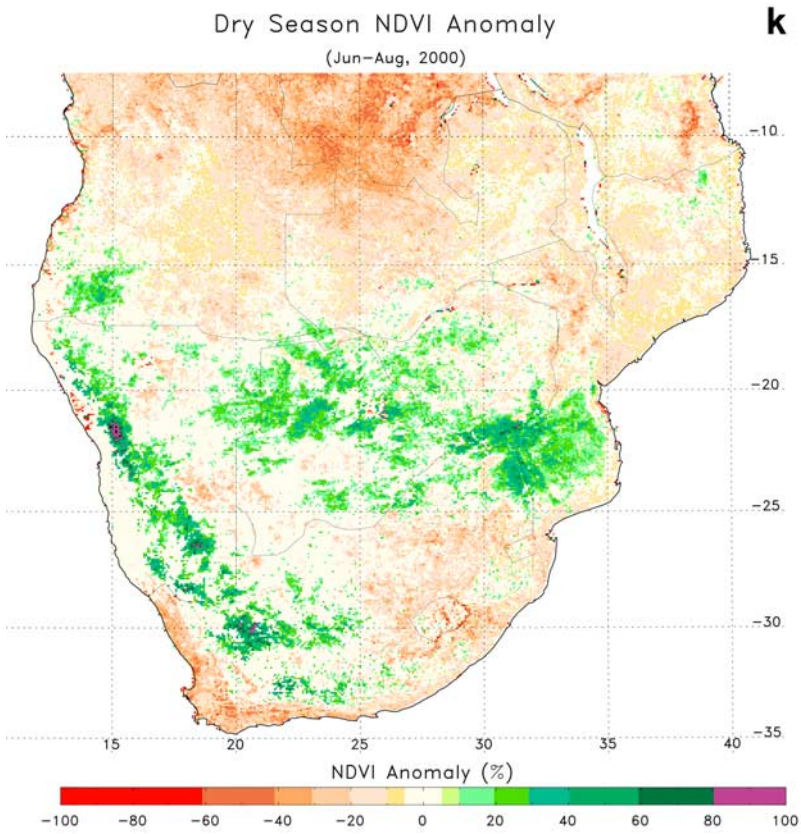

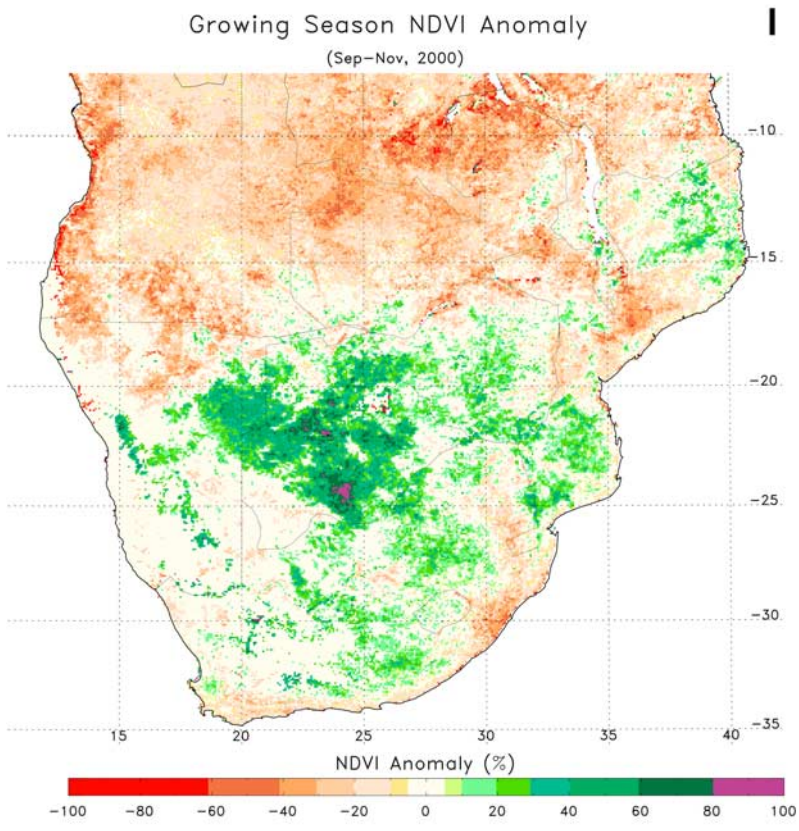

Figure 4. (continued)

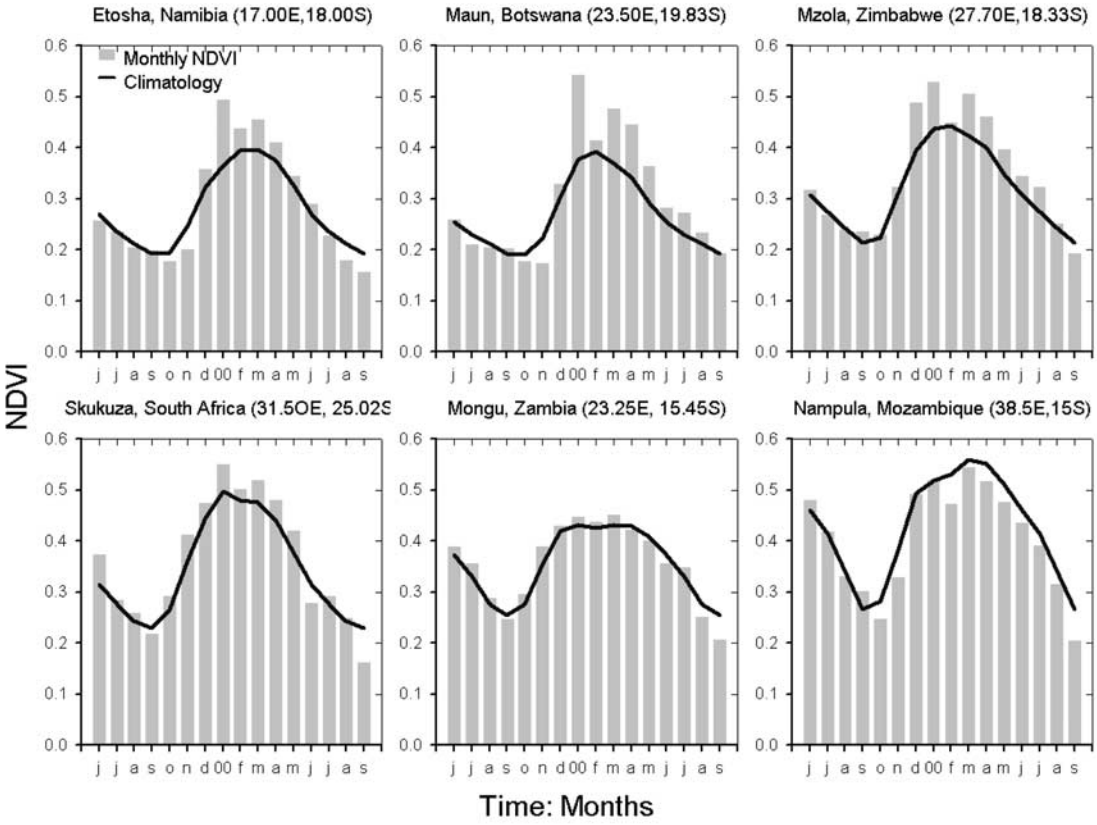

Figure 5. Long-term monthly mean (1982–1999) values of NDVI shown by the heavy solid line and monthly values shown by bar plots for SAFARI 2000 sites for the period July 1999–July 2000. During the 1999/2000 season most of the sites had above normal NDVI (Etosha, Maun, Mzola, and Skukuza) that persisted into the dry season in 2000. The other sites had near normal (Mongu) to slightly below normal (Nampula) NDVI, showing a weak to inverse relationship to ENSO at the northern extremes of the region.

compared against the respective long-term means. The upper panel shows the long-term means for December, January, February (DJF), March, April, May (MAM), June, July, August (JJA) and September, October, November (SON). The middle panel shows the actual seasonal means during this period and the lower panel shows the corresponding seasonal anomalies. In general, there is a remarkable difference between the seasonal means for 1999/2000 compared to their long-term means, especially for DJF and MAM. The 0.4 NDVI contour extended further west and southwest during the 1999/2000 season to cover most of Namibia and Botswana, where typical DJF-MAM value ranges from 0.1 to 0.2. Most of the region south of 15°S had above normal NDVI, with magnitudes of 20% over the eastern portion of the region to in some cases ~100% above their respective long-terms means. The rest of the region between 10°S and 15°S had near normal NDVI levels. The above average NDVI was due to the above normal rainfall over the region that persisted for several months beginning in November through May [see *Bell et al.*, 2000]. Some of the semiarid areas in the western portion of the region received 300mm of rainfall between December and February. The vegetation response to above normal moisture levels resulted in above normal NDVI persisting over a large portion of the region, especially in Namibia, Botswana and northern South Africa during the dry season (JJA) into the spring season (SON) (Figure 4 lower panel). The magnitude and temporal persistence of positive NDVI anomalies during this period was the highest recorded in the entire NDVI record for the region from July 1981 to June 2000 *Anyamba et al.*, 2002 (see Figure 2a). The above normal rainfall was in part due to the prevailing La Niña conditions during the 1999–2000 period, which typically leads to above normal rainfall over this region [*Bell et al.*, 2000] (see also http://www.cpc.ncep.noaa.gov/products/expert_assessment/seasonal_djf9900/index). Since this region shows the strongest teleconnection to ENSO over Africa [*Ropelewski and Halpert*, 1996], the resulting precipitation-vegetation anomalies were not totally unexpected, but the magnitude and temporal persistence of the positive NDVI anomalies surpassed other La Niña events for the NDVI time record.

5.2. Temporal Evolution Patterns

[16] The monthly NDVI values and long-term mean values for selected SAFARI 2000 sites are shown in Figure 5. The figure illustrates the NDVI monthly time series from July 1999 to September 2000. With the exception of Mongu in Zambia and Nampula in northeastern Mozambique, the monthly NDVI values for all other sites

were persistently above their long-term mean values from November 1999 to August 2000, with a peak during the height of the southern summer rainfall season, December–March. These sites are more sensitive to variability in precipitation and thus have a higher capacity for change. NDVI values for Mongu and Nampula were near normal to slightly below normal during this period. This may be because they are located in an area of weaker ENSO teleconnections (for example Nampula) as shown in Figure 2b or that the vegetation types over these two sites are less sensitive to rainfall [*Nicholson et al.*, 1990; *Tucker and Sellers*, 1986; *Fuller and Prince*, 1996]. The above normal and persistent rainfall resulted in an extended growing season as shown by above normal NDVI values during the dry season in JJA-SON 2000. The extended growing season is a typical feature of the manifestation of cold ENSO events over southern Africa, exemplified by the tendency for an extension of the rainfall season [*Nicholson and Entekhabi*, 1986].

[17] Recent studies from North American Long Term Ecological Research (LTER) sites and southern Africa affirm that the greatest interannual photosynthetic variability occurs in grassland sites with forest areas being the least variable [*Knapp and Smith*, 2001; *Scanlon et al.*, 2002]. It would appear that the same case might be stated for Mongu and Nampula, which have denser tree cover than the other sites. The grassland/shrub cover sites are more sensitive to variability in precipitation and have a larger capacity for change in production than the wet miombo woodland environments. Sensitivity to precipitation variability and hence the potential for biomass accumulation will have an impact on the spatial distribution and amount of fuel available for biomass burning and the type and amount of emissions likely to occur from one year to another.

6. Comparison Between 1991/1992 and 1999/2000

6.1. NDVI Mean and Anomaly Patterns

[18] Mean NDVI seasonal patterns and anomalies for the 1991/1992 period are shown in Figure 6. Compared to the seasonal long-term means shown in Figure 4, the 1991/1992 growing season shows much lower NDVI levels, especially during the peak period of the growing season (DJF, MAM). The 0.4 NDVI contour was located further east and north compared to its long-term position in the center of the region. During the dry season period, JJA and SON, the 0.1 NDVI contour was located further east in eastern Botswana, Zimbabwe and Mozambique, from its mean position in Namibia and western South Africa during 1991/1992. This pattern corresponds well with the accumulated rainfall for 1991/1992 (Figure 7a) and contrasts sharply with conditions during 1999/2000 (Figure 4, lower panel, Figure 7b). The anomaly patterns in 1991/1992 show below normal NDVI conditions developing over the east-central sector of the region during DJF (Figure 6). By MAM, the entire region below 15°S was dominated by below normal NDVI. In particular, the area located between 20°S and 25°S experienced NDVI departures of ~40%–60% below normal (rainfall <400 mm from July 1991–September 1992, Figure 7a). This pattern of below normal NDVI persists over the eastern side of the region during JJA and SON, reaching up to 80% below normal of NDVI during SON 1992 over a large area of Mozambique, eastern South Africa and Zimbabwe. The low rainfall in 1992 resulted in the worst drought over the region in the last 20 years. This drought, like previous droughts of 1982/1983, 1986/1987 and 1994/1995 were associated with the occurrence of a warm ENSO event, which resulted in a large rainfall deficit over most of the region. A comparison of average rainfall for the period July–September between 1991 to 1992 and 1999 to 2000 shows that most of the region received <400 mm of rainfall during the fourteen-month period in 1991/1992 compared to between 500–1200 mm during the 1999/2000 period (Figure 7).

[19] Comparisons of the monthly evolution of NDVI and rainfall at the study sites for these two time periods are shown in Figure 8. Etosha, Maun, Mzola and Skukuza consistently show that the 1991/1992 period had lower NDVI values than the 1999/2000 period, with the greatest difference being during the middle of the growing season (DJF). These sites received significantly lower rainfall in 1991/1992 compared to 1999/2000 (Figure 8 rainfall plots). On the other hand, Mongu and Nampula show quite similar evolution pattern with negligible differences in NDVI levels and rainfall amounts between the two periods. NDVI values for December–April 1991/1992 are only slightly lower for Mongu as compared to the same period in 1999/2000. Nampula shows the reverse pattern, with NDVI being slightly higher during 1991/1992 compared to 1999/2000 during the February–May period. The higher NDVI can be attributed to higher rainfall in the area around Nampula during the 1991/1992 period (Figures 7b and 8). It is apparent here that there are more marked differences in NDVI from warm to cold ENSO conditions for the dry grassland/shrubland sites located in the core area of ENSO response than for the wet miombo woodland sites or sites located at the boundary of the ENSO teleconnections to East-central Africa, such as Nampula.

6.2. NDVI-ENSO Relationships: 1991/1992 and 1999/2000

[20] Comparisons between NDVI anomalies for the sample sites and NINO3.4 SST index for the two times are shown in Figure 9. These plots show a predominant inverse relationship between NDVI/SST departures from warm ENSO conditions in 1991/1992 to cold conditions in 1999/2000. The relationship is more pronounced for the grassland/shrubland areas located within the core area of ENSO teleconnections within the region (see Figure 2b). Etosha (a), Maun (b) Mzola (c) and Skukuza (d) show a distinct inverse relationship to NINO3.4 SST, particularly during the mature phase of the warm ENSO event during January–March 1992. The temporal evolution of the anomalies shows a phase change in the middle of the warm event period. During the spring and early summer periods (September–November) Etosha, Maun, Mzola and to a small extent Skukuza, all have positive NDVI anomalies. During the mature phase of the event from December to May, there is pronounced change to negative anomalies (drought).

[21] This phase change is a known feature of the influence of the Southern Oscillation on rainfall variability in the region [*Nicholson and Entekhabi*, 1986]. It has been noted

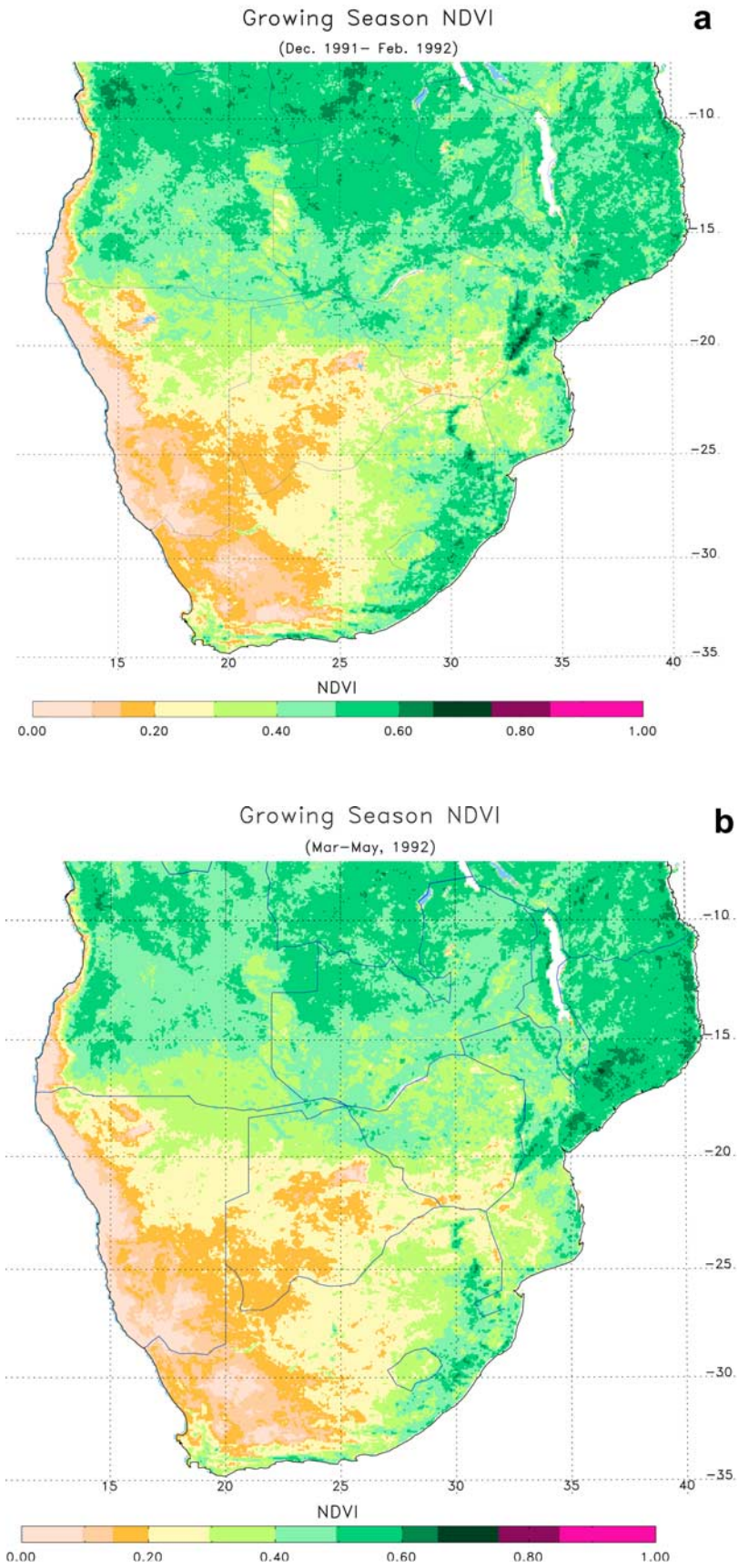

Figure 6. (a–d) Seasonal mean NDVI maps during the 1991/1992 season and (e–h) the corresponding anomalies expressed as percent departures from respective long-term means.

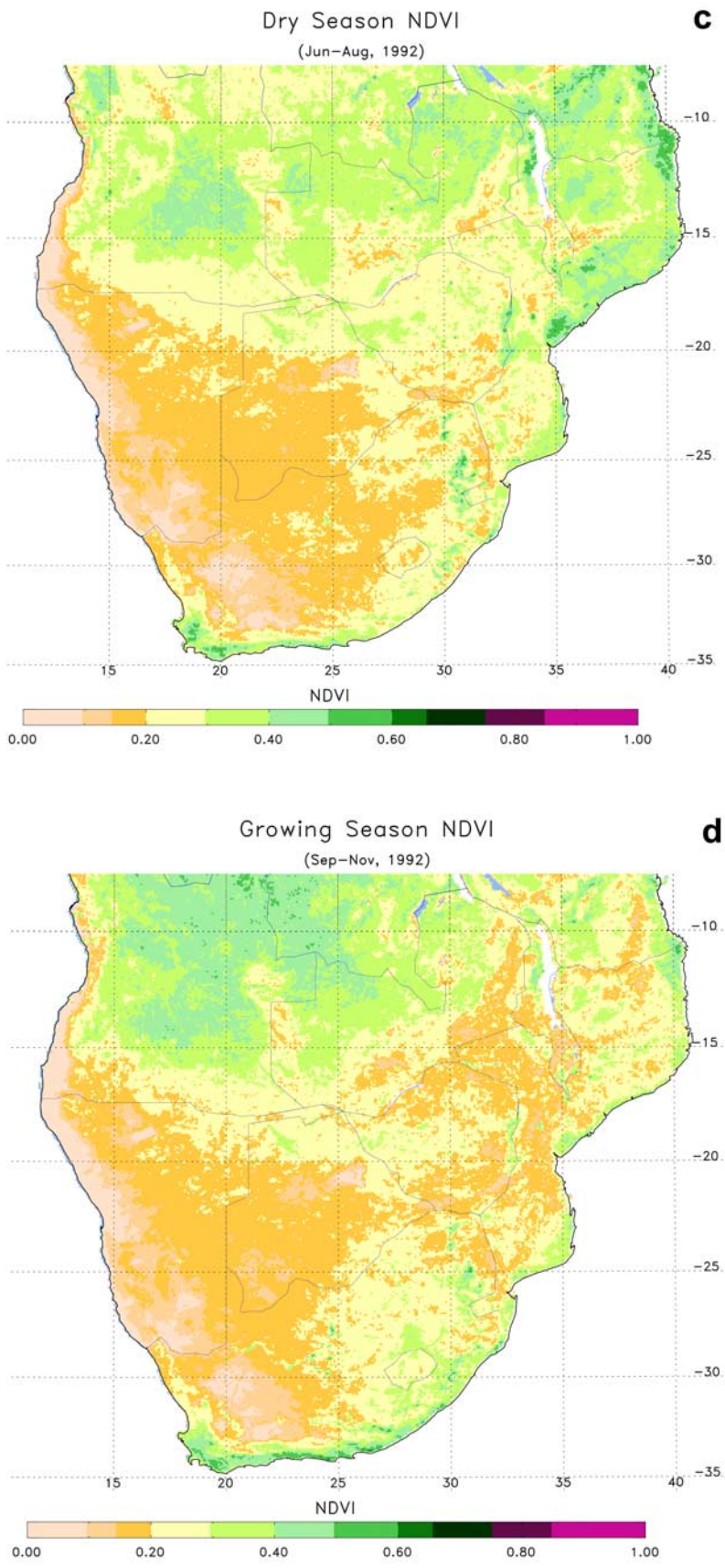

Figure 6. (continued)

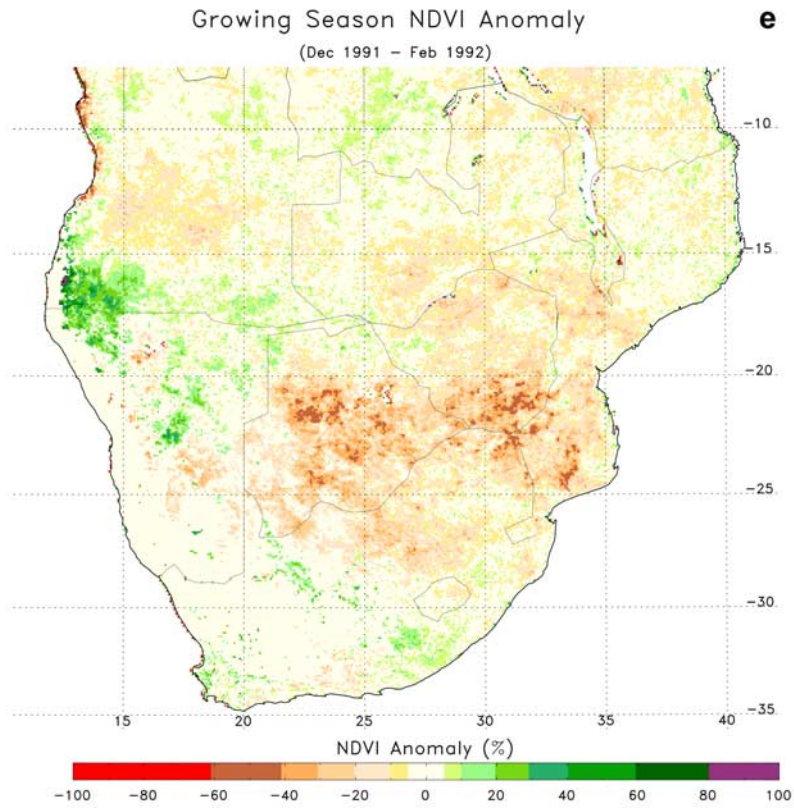

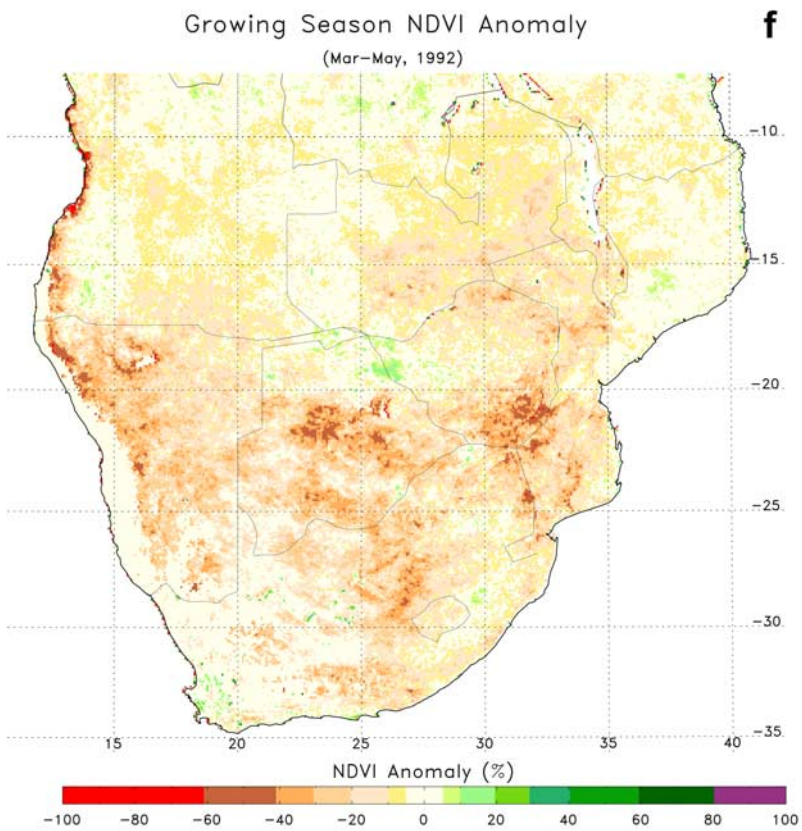

Figure 6. (continued)

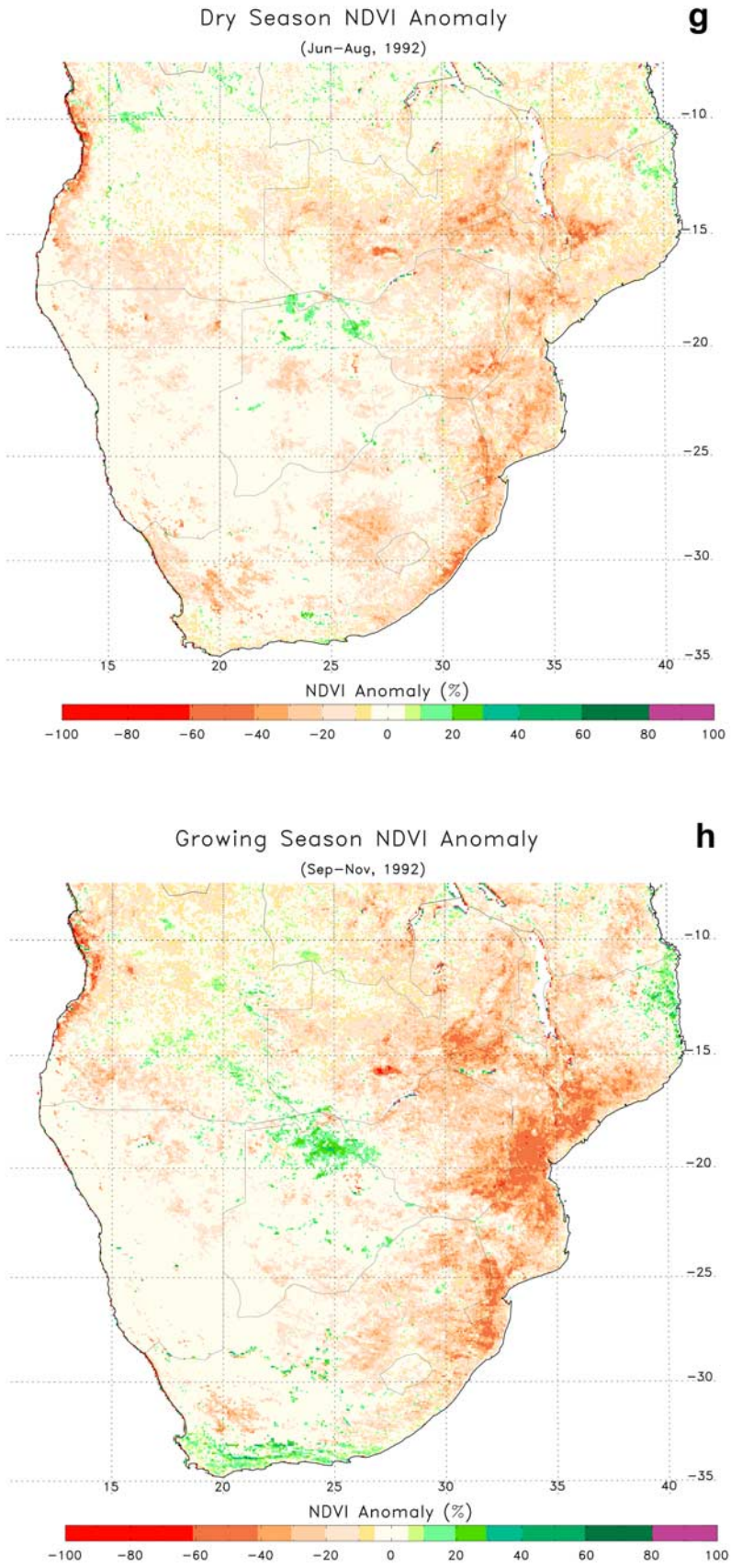

Figure 6. (continued)

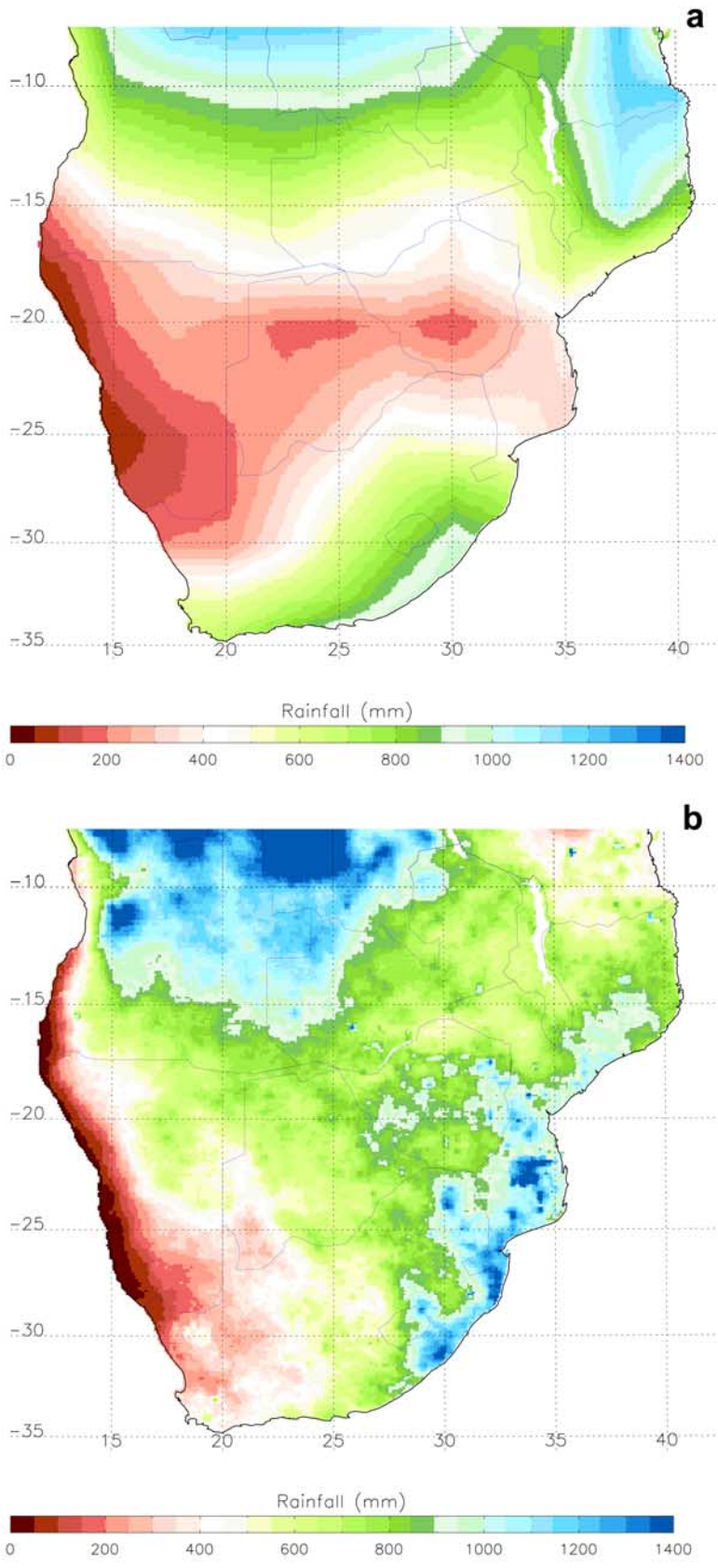

Figure 7. Accumulated rainfall for (a) July 1991–September 1992 and (b) July 1999–September 2000. During the 1991–1992, period drought conditions prevailed with most areas of the region receiving less than 400 mm of rainfall. This is contrast to the 1999–2000 period with most areas receiving between 500 and 1200 mm.

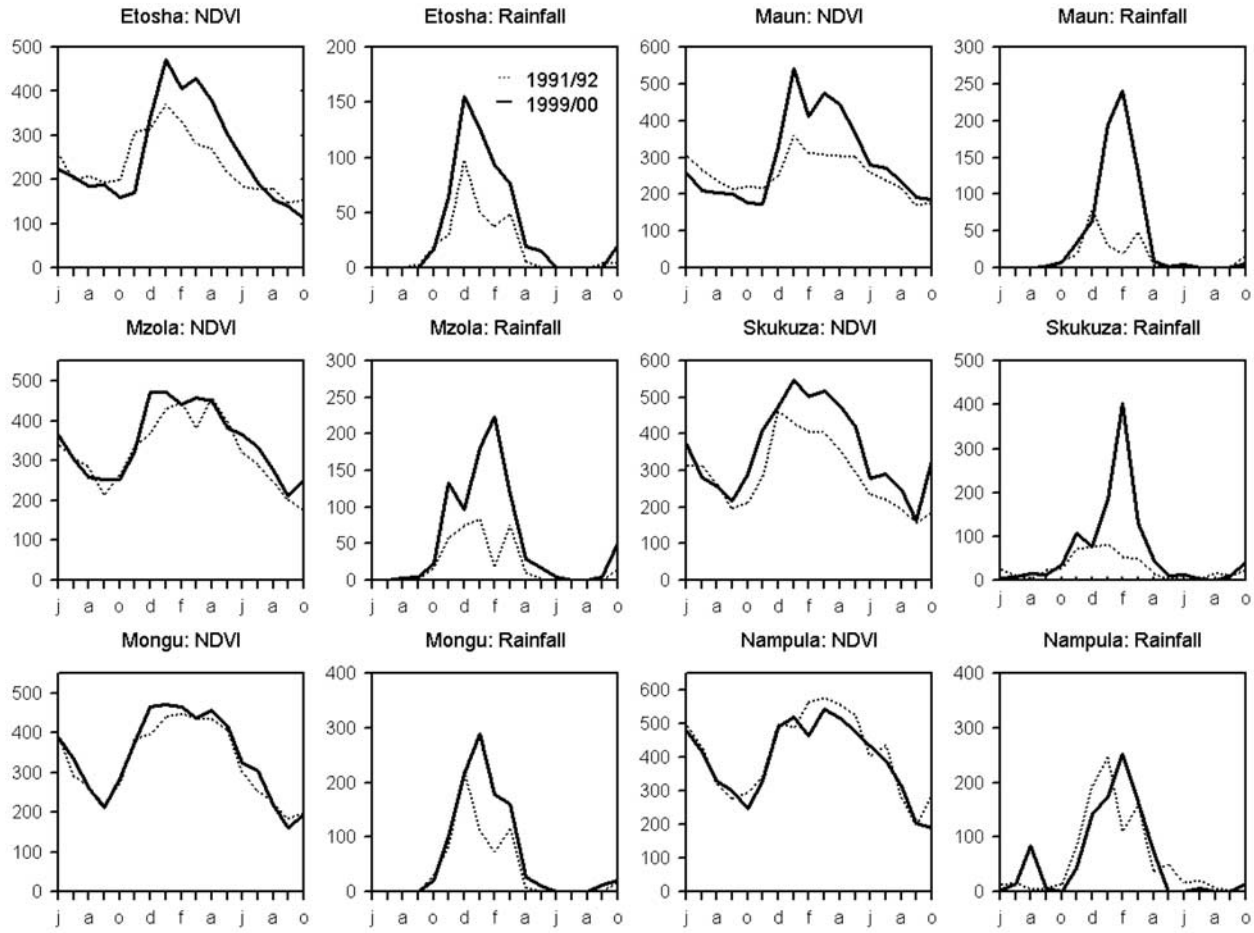

Figure 8. Comparison of temporal evolution of monthly NDVI and rainfall values for 1991/1992 (dotted lines) and 1999/2000 (thick lines) seasons. All sites except Mongu and Nampula, recorded significantly lower NDVI values during the 1991/1992 period (low rainfall, ENSO warm phase) compared to 1999/2000 (high rainfall, ENSO cold phase).

that during the early phase of a developing warm event there is a tendency for above normal precipitation, which shifts to below normal precipitation during the mature phase. It is apparent here that the vegetation pattern maintains this memory of the temporal evolution of rainfall during the warm event in 1991/1992. The other sites (Mongu and Nampula) do not show such a pattern, indicating a weak response of vegetation at these sites to this ENSO warm event. During the cold event in 1999/2000, all the sites except Nampula show positive anomalies in NDVI (inversely related NINO3.4 SST index). Maximum positive NDVI anomalies occurred during the mature phase of the cold event (December–March). The positive anomalies propagated into May–July, but declined as the SST increased. In general, while there may be a lagged vegetation response to ENSO forced rainfall variability over the region [*Nicholson et al.*, 1990; *Ricard and Poccard*, 1998], the evolution of the vegetation patterns shown strongly illustrates the inverse relationship between ENSO and interannual vegetation variability, especially for those areas located in the core area of ENSO teleconnections. This variability in SST, rainfall and photosynthetic activity is bound to influence aggregate regional biomass production and hence the amount of fuel available for burning.

7. A Comparison of Fire Occurrence in 1992 and 2000

[22] Active fires can be detected using the 3.9 μm channel of the NOAA AVHRR [*Giglio et al.*, 1999]. Daily AVHRR 1 km data from May to October were used to derive active fire distributions for the 2000 dry season (Figure 10a). The distribution of fires as detected by the AVHRR extends across the entire southern Africa region, with high concentrations in Angola, Zambia, southern Democratic Republic of Congo, western Tanzania and central Mozambique. Fires were also detected in Zimbabwe, Botswana, northeast Namibia and eastern South Africa. The fires occur in the miombo woodlands, savannas and grasslands and are a combination of fires set for land management and wildland fires [*Frost*, 1998]. In the work of *Kendall et al.* [1997], the same fire detection approach was applied to AVHRR 1 km data during the SAFARI 1992 burning season. The distribution of fires for 2000 exhibits rather different characteristics from those shown in 1992 (Figure 10b). During 2000,

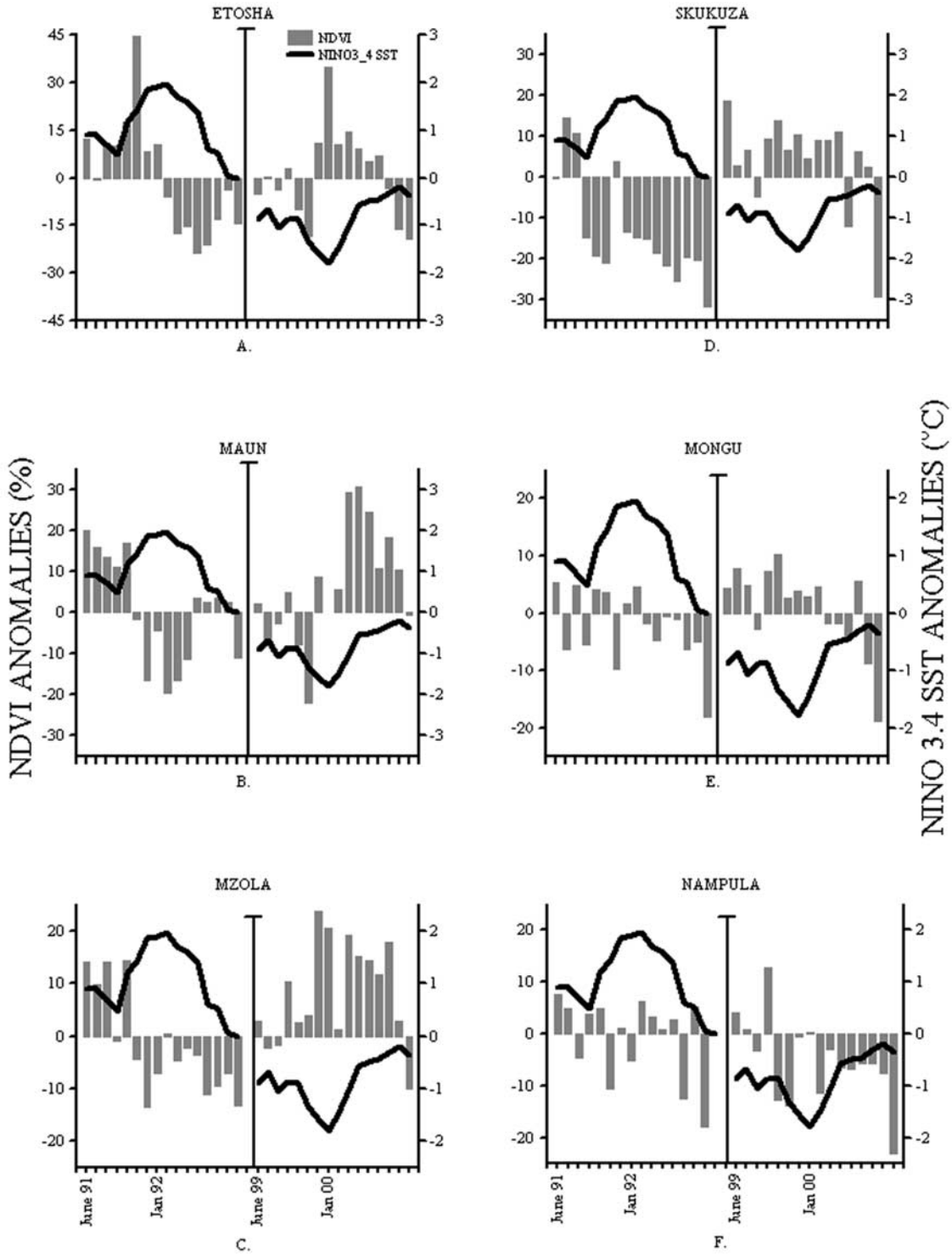

Figure 9. Time series of NDVI anomalies for selected SAFARI 2000 validation sites plotted against and NINO3.4 SST anomalies during ENSO events in 1991/1992 (warm) and 1990/2000 (cold).

there were considerably more fires over the southern part of the region, particularly in Namibia, Botswana, Mozambique and South Africa. Large differences can be seen in southern Mozambique. These differences closely match the differences in the rainfall data for the two years (Figures 7 and 8) and the NDVI anomalies shown in Figures 4 and 6. Above normal rainfall during the 1999/2000 resulted in an increase in vegetation biomass production, extending further south into the semiarid parts of the region. This provided abundant fuel for burning during the dry season. The drought in 1992 resulted in diminished vegetation production, and insufficient fuel to burn in the drier parts of Namibia,

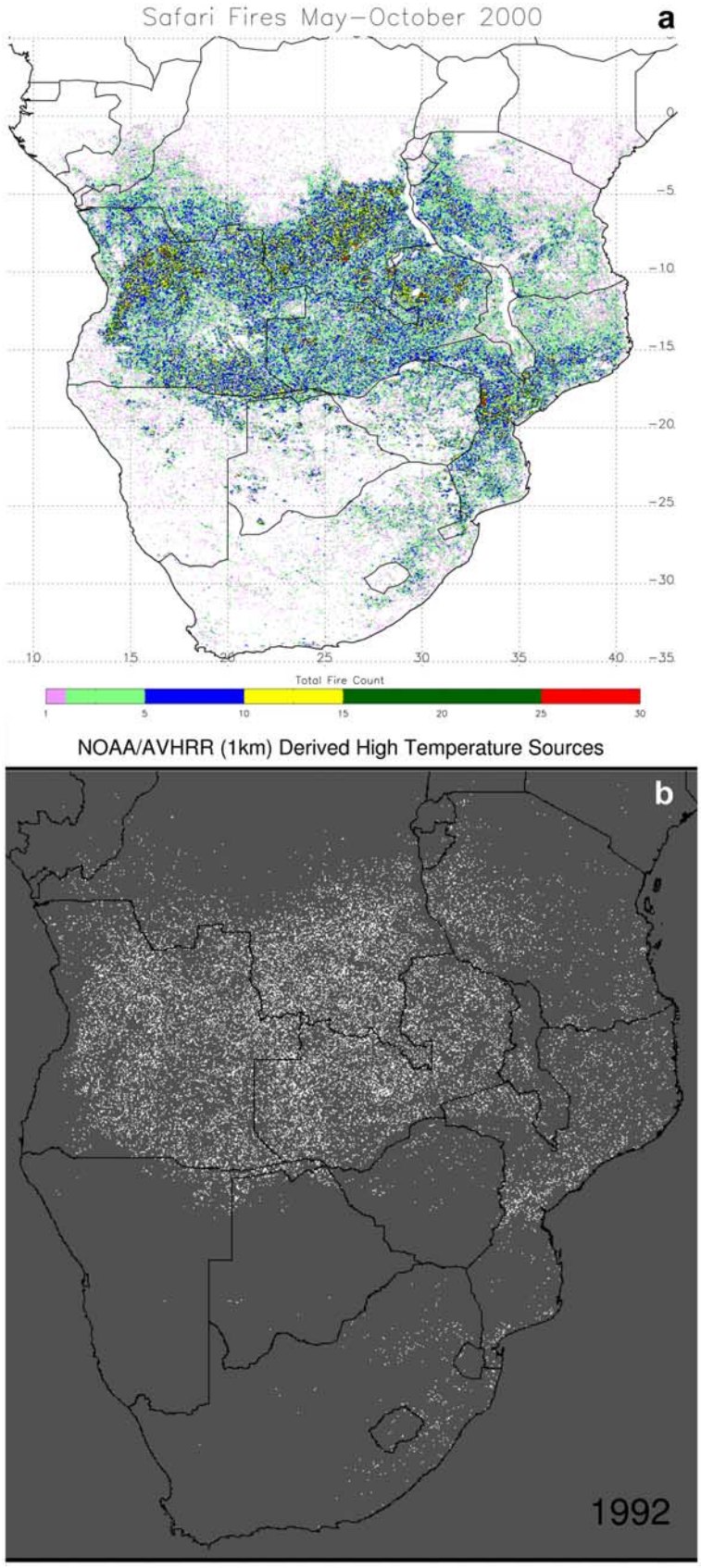

Figure 10. Spatial distribution of accumulated fire counts over southern Africa during the period (a) May–October for 2000 and (b) May to October 1992 [after *Kendall et al.*, 1997]. The spatial extent of fires increased southward during the 2000 dry season following above normal rainfall and NDVI compared to the 1992 period when drought prevailed over the region.

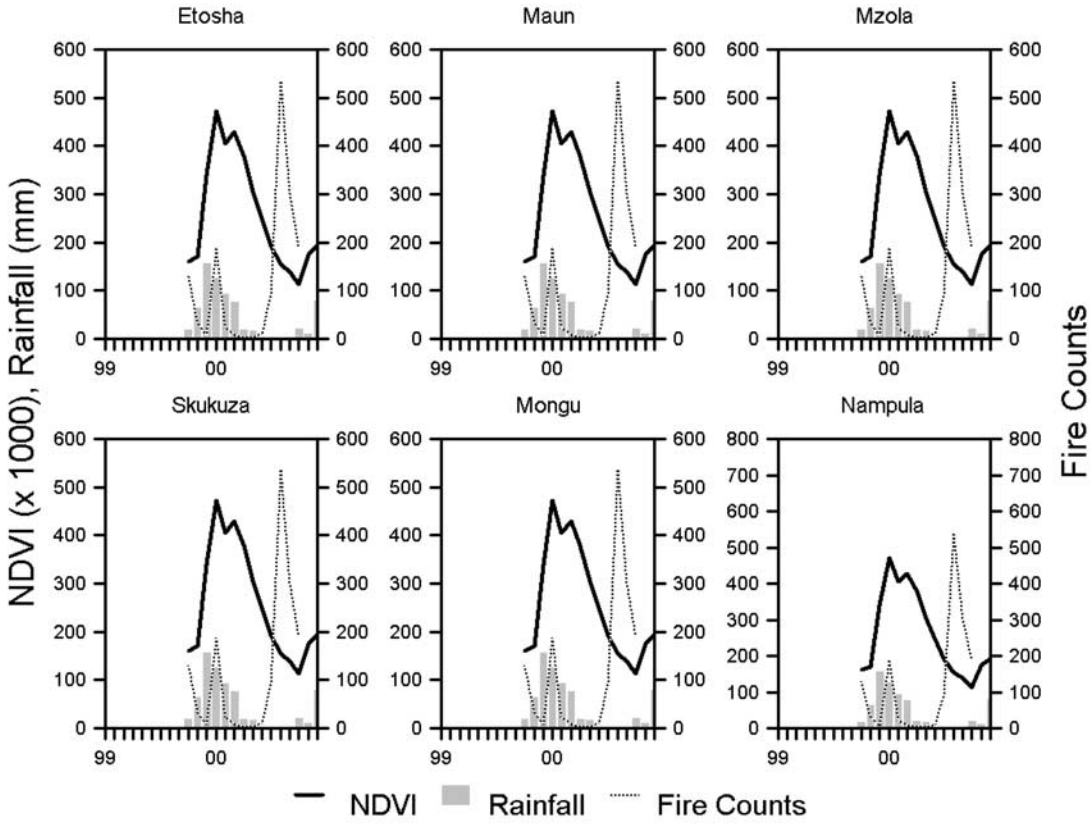

Figure 11. Temporal evolution of rainfall (mm), NDVI (×1000) (left axis) and fire activity counts (right axis) at selected SAFARI 2000 validation sites from June 1999 to October 2000.

Botswana, southern Zimbabwe and southern Mozambique. This comparison shows greater differences than were presented for the 1989 and 1992 fire seasons, particularly in southern Mozambique and southern Zimbabwe and Namibia [see *Kendall et al.*, 1997].

[23] The temporal evolution of monthly fire counts, NDVI and rainfall from October 1999 to October 2000 are shown for the 100 km square area centered on the six study areas used previously (Figure 11). All sites show an inverse relationship between the seasonality of NDVI and that of the fire counts. In general, the senescent phase of vegetation marks the beginning of the fire season, with maximum in NDVI roughly corresponding to the minima in fire occurrence and vice versa. The plot for Etosha shows the vegetation index rapidly increasing from December and peaking in January–March following the rains and fire counts starting in June, peaking in August, and then decreasing to October. Maun shows a small increase in fire counts in January, similar to Etosha but with the major increase in fires starting later in August and still increasing by October. The Mzola site shows a steady decrease in fire counts from October to December 1999 with the 2000 fire season starting in August, peaking in July and still increasing in October. Although this particular fire data set ends in October, anecdotal accounts of the 2000 fire season indicated a continuation of the burning season through to December in some parts of the region. The plot for Skukuza shows a start to the burning season in June with a peak in August, though even by October the number of fire counts is still close to the peak. It is significant to note that, Skukuza which received the highest amount of rainfall in February 2000 (~400 mm), recorded the largest number of fires at peak burning period in September 2000 (~580 fires) The plot for Mongu shows a peak NDVI in March–April, the start of the burning season in June and with the peak in fire activity in September. The Nampula site shows a large number of fires burning October–December 1999 fire season and starting six months later in June to peak in September 2000, when the highest numbers of fires are detected. The vegetation index starts to decline in May, which is later than for the other sites. These plots show that the burning season started at least halfway through the senescent phase of the NDVI curve after the end of the rain season, when the vegetation was dry enough to burn. Three of the sites (Etosha, Skukuza and Maun) all indicate a secondary fire count peak in January 2000, which is likely the result of burning of biomass accumulated during the early phase of the growing season following the rains in late 1999. This would suggest that the slight drop in NDVI in January 2000 at these three sites is likely related to fire activity. In all these instances, this secondary peak in fires follows the peak in rainfall and a secondary peak in NDVI.

8. Conclusions

[24] In this paper, we have shown that the southern Africa region exhibits high interannual variability in vegetation amount and distribution. At the short timescale, variations

in NDVI are associated with extreme interannual variability in rainfall associated in part with ENSO phenomena. El Niño and La Niña events in the region frequently result in extreme rainfall departures, with a resultant impact on vegetation state and amount and the associated vegetation index patterns. In general, the variability in NDVI is on the order of ±40% between ENSO cold and warm phases. During the 2000 growing season, above normal rainfall over the region south of 15°S resulted in NDVI levels between 10 to 90% above normal, with the largest positive departures over the western part of the region, which is predominantly semiarid. The magnitude of positive NDVI departures during this period not only surpassed the departures during the last strong ENSO cold episode in 1988/1989 but also the historical NDVI record since 1981. Above normal rainfall resulted in an extended growing season and a persistence of high NDVI conditions into the dry season (June–August). While in general the abundant rainfall was in part associated with the tropical wide, changes related to ENSO, to a large extent this was amplified by above normal SST in the southwestern Indian Ocean and the southern Atlantic Ocean surrounding southern Africa [*Bell et al.*, 2000; *Anyamba et al.*, 2002]. SSTs were above normal by approximately +1.5°C. The above normal SSTs in the southwestern Indian Ocean coupled with strong easterly winds enhanced the monsoon circulation over the region, resulting in anomalous above normal rainfall and above normal NDVI [*Anyamba et al.*, 2002]. The greatest increase in vegetation was predominantly in the semiarid grassland-shrubland western half of the region, which is most sensitive to precipitation variations.

[25] The vegetation anomaly patterns in 2000 contrasted sharply with conditions during the 1992 field campaign, when drought spread throughout the region. In 1992, the NDVI was 30–40% below normal for most of the region especially during the height of the growing season (January–March). The pattern of vegetation production and the vegetation moisture content determine the extent and distribution of fire and the number of fires in the region as a whole. In 1992, the fires were limited to the wetter northern half of the region, where miombo woodlands are dominant and the wetter areas of eastern South Africa, which provide enough fuel for burning even in this extremely dry year. The spatial extent of the fires expands during wet years. As illustrated here, during the 2000 campaign, fires occurred in the more semiarid parts in western South Africa, large areas of Botswana and Namibia dominated by savanna grassland and shrublands. Abundant and widespread rainfall resulted in an increase in the vegetation biomass providing enough fuel for fires throughout the dry season and into the beginning of the 2000/2001 growing season. Spatially, interannual variability in rainfall and hence vegetation abundance results in different geographies of fire distribution, with wetter years (1988/1989, 1999/2000) resulting in more widespread fires over the southern part of the region and dry years (1991/1992) resulting in fires limited to the northern half of the region.

[26] We can infer from these results that although there is a regional atmospheric gyre, which circulates the emissions products around the region [*van Wilgen et al.*, 1997], it is likely that airborne emissions measurements in the southern part of the region are likely to be different between 1992 and 2000. Comparison of the airborne measurements between the two campaigns as they relate to differences in fire timing and distribution will provide a better understanding of regional fire emissions. To improve our understanding of internannual variability of fires in relation to vegetation dynamics over the region, it would be useful to reprocess a continuous and consistent time series of 1 km-satellite fire measurements over the region. The 1 km record of AVHRR data collected by the South African ground receiving station in Hartebeesthoek dates from 1985 to the present. In addition, the improved active fire data sets and burned area products from new moderate instruments such as MODIS, should be used to explore the interannual variability of fire and the relationship to vegetation production and associated emissions [*Justice et al.*, 2002]. Given the apparent strong relationships between precipitation, vegetation production and fire distribution and extent, regional seasonal climate forecasts now carried out by the International Research Institute for Climate Prediction (IRI) [*Mason et al.*, 1999] could lead to improved projection of vegetation biomass conditions during the burning season, the distribution and extent of fires and the aerosol distribution over the region.

[27] **Acknowledgments.** The authors would like to thank Jackie Kendall for organizing and generating the AVHRR fire data both for 1992 and 2000, GIMMS group (NASA/GSFC) for providing the AVHRR vegetation index data, and NOAA/CPC, USAID/FEWS Project and TRMM Project for providing rainfall data used in this study.

References

Adler, R. F., G. J. Huffman, D. T. Bolvin, S. Curtis, and E. J. Nelkin, Tropical rainfall distributions determined using TRMM combined with other satellite and rain gauge information, *J. Appl. Meteorol.*, *39*(12), 2007–2023, 2000.

Anyamba, A., and J. R. Eastman, Interannual variability of NDVI over Africa and its relationship to El Niño/Southern Oscillation, *Int. J. Remote Sens.*, *17*, 2533–2548, 1996.

Anyamba, A., C. J. Tucker, and J. R. Eastman, NDVI anomaly patterns over Africa during the 1997/98 ENSO warm event, *Int. J. Remote Sens.*, *22*(10), 1847–1859, 2001.

Anyamba, A., C. J. Tucker, and R. Mahoney, El Niño and La Niña: Vegetation response patterns over east and southern Africa 1997–2000, *J. Clim.*, *15*(21), 3096–3103, 2002.

Asrar, G., M. Fuchs, E. T. Kanemasu, and J. L. Hatfield, Estimating absorbed photosynthetic radiation and leaf area index from spectral reflectance in wheat, *Agron. J.*, *76*, 300–306, 1984.

Bell, G. D., S. M Halpert, R. C. Schnell, R. W. Higgins, J. Lawrimore, V. E. Kousky, R. Tinker, W. Thiaw, M. Chelliah, and A. Artusa, Climate assessment for 1999, *Bull. Am. Meteorol. Soc.*, *8*, 13282000.

Cihlar, J., L. St. Laurent, and J. A. Dyer, The relation between normalized difference vegetation index and ecological variables, *Remote Sens. Environ.*, *35*, 279–298, 1991.

Eastman, J. R., and A. Anyamba, Prototypical patterns of ENSO-related drought and drought precursors in southern Africa, paper presented at The Thirteenth Pecora Symposium Proceedings, Am. Soc. of Photogramm. and Remote Sens., Sioux Falls, S. D., 2 –22 Aug. 1996.

Eastman, J. R., and M. A. Fulk, Long sequence time series evaluation using standardized principal components analysis, *Photo. Eng. Remote Sens.*, *53*, 1649–1658, 1993.

Frost, P., Fire in southern African woodlands: Origins, impacts, effects and controls, FAO meeting on public policies affecting forest fires, *FAO Forest. Pap. 138*, pp. 181–207, United Nations Food and Agric. Org., Rome, 1998.

Fuller, D. O., and S. D. Prince, Rainfall and foliar dynamics in tropical southern Africa: Potential impacts of global climatic change on savanna vegetation, *Clim. Change*, *33*, 69–96, 1996.

Giglio, L., J. D. Kendall, and C. O. Justice, Evaluation of global fire detection algorithms using simulated AVHRR infrared data, *Int. J. Remote Sens.*, *20*, 1947–1985, 1999.

Gray, T. I., and D. B. Tapley, Vegetation health: Natures climate monitor, *Adv. Space Res.*, *5*, 371–377, 1985.

Herman, A., V. B. Kumar, P. A. Arkin, and J. V. Kousky, Objectively determined 10-day African rainfall estimates created for famine early warning systems, *Int. J. Remote Sens.*, *18*, 2147–2159, 1997.

Holben, B. N., Characteristics of maximum-value composite images for temporal AVHRR data, *Int. J. Remote Sens.*, *7*, 1417–1434, 1986.

Huete, A. R., Spectral response of a plant canopy with different soil backgrounds, *Remote Sens. Environ.*, *17*, 37–53, 1985.

Huffman, G. J., R. F. Adler, B. Rudolf, U. Schneider, and P. R. Keehn, Global precipitation estimates based on a technique for combining satellite-based estimates, rain gauge analysis, and NWP model precipitation information, *J. Clim.*, *8*, 1284–1295, 1995.

Janowiak, J. E., An investigation of interannual rainfall variability in Africa, *J. Clim.*, *1*, 240–255, 1988.

Jury, M. R., H. R. Valentine, and J. R. E. Lutjeharms, Influence of the Agulhas Current on summer rainfall along the southeast coast of South Africa, *J. Appl. Meteorol.*, *32*, 1282–1287, 1993.

Justice, C. O., B. N. Holben, and M. D. Gwynne, Monitoring east African vegetation using AVHRR data, *Int. J. Remote Sens.*, *7*, 1453–1474, 1986.

Justice, C. O., T. F. Eck, D. Taure, and B. N. Holben, The effect of water vapor on normalized difference vegetation index derived for the Sahelian region from NOAA AVHRR data, *Int. J. Remote Sens.*, *12*, 1165–1187, 1991.

Justice, C. O., L. Giglio, S. Korontzi, J. Owens, J. T. Morisette, D. Roy, J. Descloitres, S. Alleaume, F. Petitcolin, and Y. Kaufman, The MODIS fire products, *Remote Sens. Environ.*, *83*, 244–262, 2002.

Kendall, J. D., C. O. Justice, P. R. Dowty, C. D. Elvidge, and J. G. Goldammer, Remote sensing of fires in southern Africa during the SAFARI 1992 campaign, in *Fire in Southern Africa Savannas: Ecological and Atmospheric Perspectives*, edited by B. W. van Wilgen et al., pp. 89–130, Witwatersrand Univ. Press, Johannesburg, 1997.

Knapp, A. L., and M. D. Smith, Variations among biomes in temporal dynamics of above ground biomass, *Science*, *291*(5503), 481–484, 2001.

Lindsey, J. A., Southern Africa rainfall, the southern oscillation, and a Southern Hemisphere semi-annual cycle, *J. Climatol.*, *8*, 17–30, 1988.

Los, S. O., Calibration adjustment of the NOAA AVHRR normalized difference vegetation index without recourse to channel 1 and 2 data, *Int. J. Remote Sens.*, *14*, 1907–1917, 1993.

Mason, S. J., and J. A. Lindesay, A note on the modulation of the southern oscillation-South African rainfall associations with the quasi-biennal oscillation, *J. Geophys. Res.*, *98*(D5), 8847–8850, 1993.

Mason, S. J., L. Goddard, N. E. Graham, E. Yulaeva, L. Sun, and P. A. Arkin, The IRI seasonal climate prediction system and the 1997/98 El Niño event, *Bull. Am. Meteorol. Soc.*, *80*, 1853–1873, 1999.

Myneni, R. B., S. O. Los, and C. J. Tucker, Satellite-based identification of linked vegetation index and sea surface temperature anomaly areas from 1982–1990 for Africa, Australia and South America, *Geophys. Res. Lett.*, *23*, 729–732, 1996.

Nicholson, S. E., and D. Entekhabi, The quasi-periodic behavior of rainfall variability in Africa and its relationship to the southern oscillation, *Arch. Meteorol. Geophys. Bioklimatol. A*, *34*, 311–348, 1986.

Nicholson, S. E., M. L. Davenport, and A. R. Malo, A comparison of vegetation response to rainfall in the Sahel and east Africa using normalized difference vegetation index from NOAA-AVHRR, *Clim. Change*, *17*, 209–241, 1990.

Reason, C. J. C., Subtropical Indian Ocean SST dipole events and southern Africa rainfall, *Geophys. Res. Lett.*, *28*(11), 2225–2227, 2001.

Ricard, Y., and I. Poccard, A statistical study of NDVI sensitivity to seasonal and interannual rainfall variations in southern Africa, *Int. J. Remote Sens.*, *19*, 2907–2920, 1998.

Ropelewski, C. F., and M. S. Halpert, Quantifying southern oscillation-precipitation relationships, *J. Clim.*, *9*, 1043–1059, 1996.

Scanlon, T. M., J. D. Albertson, K. K. Caylor, and C. A. Williams, Determining land surface fractional cover from NDVI and rainfall time series for a savanna ecosystem, *Remote Sens. Environ.*, *82*(2–3), 376–388, 2002.

Scholes, R. J., D. Ward, and C. O. Justice, Emissions of trace gases and aerosol particles due to vegetation burning in Southern Hemisphere Africa, *J. Geophys. Res.*, *101*, 23,677–23,682, 1996.

Sellers, P. J., Canopy reflectance, photosynthesis and transpiration, *Int. J. Remote Sens.*, *8*, 1335–1372, 1985.

Townshend, J. R. G., and C. O. Justice, Analysis of the dynamics of African vegetation using the normalized difference vegetation index, *Int. J. Remote Sens.*, *7*, 1435–1446, 1985.

Tucker, C. J., Red and photographic infrared linear combinations for monitoring vegetation, *Remote Sens. Environ.*, *8*, 127–150, 1979.

Tucker, C. J., and P. J. Sellers, Satellite remote sensing of primary production, *Int. J. Remote Sens.*, *7*, 1133–1135, 1986.

Tucker, C. J., W. W. Newcomb, and H. E. Dregne, AVHRR data sets for determination of desert spatial extent, *Int. J. Remote Sens.*, *17*, 3547–3565, 1994.

van Wilgen, B. W., M. Andreae, J. Goldammer, and J. A. Lindesey (Eds.), *Fire in Southern Africa Savannas: Ecological and Atmospheric Perspectives*, 256 pp., Witwatersrand Univ. Press, Johannesburg, 1997.

Vermote, E. F., N. Z. El Saleous, C. O. Justice, Y. J. Kaufman, J. Privette, L. Remer, J. C. Roger, and D. Tanré, Atmospheric correction of visible to middle infrared EOS-MODIS data over land surface, background, operational algorithm and validation, *J. Geophys. Res.*, *102*, 17,131–17,141, 1997.

Walker, N. D., Links between South African summer rainfall and temperature variability of the Agulhas and Benguela current systems, *J. Geophys. Res.*, *95*(C3), 3297–3319, 1990.

A. Anyamba, Goddard Earth Science Technology Center, University of Maryland, Baltimore County and NASA Goddard Space Flight Center, Biospheric Sciences Branch, Greenbelt, MD 20771, USA. (assaf@ltpmail.gsfc.nasa.gov)

C. O. Justice, Department of Geography, 2181 Lefrak Hall, University of Maryland, College Park, MD 20742, USA. (justice@hermes.geog.umd.edu)

R. Mahoney, Global Science and Technology, 6411 Ivy Lane Suite 300, Greenbelt, MD 20770, USA. (mahoney@mombasa.gsfc.nasa.gov)

C. J. Tucker, NASA Goddard Space Flight Center, Biospheric Sciences Branch, Code 923.0, Greenbelt, MD 20771, USA. (compton@ltpmail.gsfc.nasa.gov)